DEF damage in heat cured mortars made of recycled concrete sand aggregate

Alexandre Yammine, Nordine Leklou, Marta Choinska, François Bignonnet, Jean-Michel Mechling

DEF damage in heat cured mortars made of recycled concrete sand aggregate

Alexandre YAMMINE[a,*], Nordine LEKLOU[a], Marta CHOINSKA[a], François BIGNONNET[a] and Jean-Michel MECHLING[b].

[a]University of Nantes - IUT Saint-Nazaire, GeM, CNRS UMR 6183, Research Institute in Civil Engineering and Mechanics, France.

[b]Université de Lorraine, Institut Jean Lamour 7198, Nancy, F54000, France

[*]Corresponding author: Alexandre YAMMINE, email: alexandre.yammine@univ-nantes.fr

Abstract

The purpose of this study is to investigate DEF development in heat cured mortars made of recycled sand aggregate with sodium sulphate or gypsum plaster powder additions to stimulated DEF development. Ten different formulations have been studied for more than a year. DEF damage comparison between different mortars made of RCA sand and standardised siliceous sand is made with or without sulphate addition. Sodium sulphate was used in three formulations at 5% of total SO_3 by cement weight, while gypsum plaster powder was used in four formulations with two different fineness (<0.1 mm and 0.1-2 mm) and contents (1.2% and 0.8% of sulphate content in sand) to simulate a scenario of recycled aggregate pollution by gypsum plaster during the demolition phase. Three other mortars were formulated without any addition to determine the impact of sulphate addition. Sodium sulphate was found to induce and amplify DEF. Gypsum plaster powder did not enhance damage and both mortars made of recycled sand with or without gypsum addition showed little differences concerning DEF expansion. RCA based mortars had lower DEF damage than siliceous reference sand based mortars. This result is explained by air entrainment effect of RCA sands and to a lesser extent by chemical differences between mortars made of recycled and siliceous sand. Hence, DEF damage should be further studied at sulphate and alkaline content far above the current standard limits for RCA based concretes.

Keywords: delayed ettringite formation (DEF), mortar, damage, recycled concrete aggregates (RCA), heat curing, sulphate, expansion, permeability, porosity, scanning electron microscope (SEM).

1. Introduction

DEF related problems in concretes incorporating RCA are not yet established and this is related to the novelty of RCA industry. Replacing natural aggregates (NA) with RCA will increase in the future and higher replacement amounts will be allowed in newer standards. Construction and demolition waste (CDW) disposal is an environmental problem that could be solved by recycling CDW [1]. Whereas on the one hand, natural aggregates are having a critical shortage [2], on the other hand, demolished concrete quantities are increasing [3] and quarries are increasingly moving away from the cities where aggregates should be transported to be used [4]. The replacement of NA by RCA will diminish environmental impact generated by quarry exploitation and solve the problem of demolished concrete disposal estimated about several million tons per year [5].

Delayed ettringite formation (DEF) is a reaction consisting of a retarded formation of ettringite mineral that normally crystalizes during cement hydration, which could likely lead to swelling and cracking of concrete. Ettringite decomposition induced by early elevated temperature above 70°C is the main reason for DEF development [6–9]. More stable products are produced by this decomposition and are absorbed by C-S-H. They can be released later to form ettringite crystals in the hardened matrix [10,11]. Humidity and water exposure enable ions exchange and ions leaching from concrete [12]. Water availability enables ettringite

recrystallization in the existent porosity inducing crystallization pressure and leading to damage. DEF risk is serious in heat exposed concrete mainly in self-heated concrete during massive casting or in case of thermal cure in precast elements [13,14]. Many factors are implicated in DEF development, they are divided into four main categories: thermal condition, composition of the cementitious material, environment and microstructure [15–17]. Many studies have established a direct link between different factors and DEF. Zhang et al. found that cement sulphate and aluminate content should be equal to induce the highest expansion, alkali content is well noted as an important factor [18]. Nevertheless, the study stated that other factors are implicated in DEF. Porosity and microcracking of the material are also important, higher porosity and microcracking is linked to earlier DEF by allowing moisture to penetrate in the microstructure [7,19]. Humidity and water exposure are found to influence damage initiation and intensity. Renewed water exposure leaches hydroxide ions leading to more ettringite stability and crystallization which leads to more expansion and cracking [20]. Aggregate type plays a very important role, siliceous aggregates are more sensitive to DEF than limestone aggregates [21].

Regarding our study, there is a lack of sight in the durability of concrete made from RCA. In general, higher porosity and water absorption, lower density, higher alkali, sulphate and chloride contents are found in RCA in comparison to natural aggregates [5,22,23]. It was found that small RCA particles have greater water absorption and porosity due to their larger paste amount [22].

According to the European standard [NF EN 206/CN, 2014], the maximum authorized RCA gravel quantity in concrete should not exceed 60% by weight of total aggregates for the highest RCA quality and the lowest aggressive environment (X0 exposition class: extremely low dryness; see Table 1) [24]. The limit is only 30% by weight of total aggregates for moderately aggressive environment (XC1 and XC2 exposition classes). Moreover, RCA sand substitution is completely prohibited for all environmental expositions except for the X0 one for which a maximum limit of 30% by weight of sand is allowed.

Studies on RCA has shown that most soluble sulphates come from finely dispersed gypsum during the demolition [5]. Gypsum plaster is the main material used in construction which is integrally composed from gypsum. Removing plaster from RCA is found to be a difficult task and significant quantities remain during the sorting leading to sulphate pollution. Silva et al. [5] found that sulphate content is in almost all the recycled aggregates in the range of 0.1% to 1%. The European standard [NF EN 12620] restricts sulphate to 0,2% bwa (by weight of aggregate) in case of sulphate attack risk [25], and no limit in case of low probability of sulphate reaction. Sulphate should be determined according to the norm NF EN 1744-1 [26]. Other norms have allowed higher values, 0.8% bwa is the maximum limit of the Spanish code [27] and 1% bwa is the maximum limit for the British code [28]. Concerning DEF risks in cementitious material using RCA, two studies in "RECYBETON" project [29] have tested several concretes and mortars incorporating different fractions of RCA. Sulphate RCA content was between 0.3% and 0.6% in sands, gypsum plaster was used to simulate sulphate pollution from 0.8% to 1.2% bwa. The two studies found no DEF risk when RCA are partially incorporated till 60% of total aggregate weight. Alkali content was found to impact DEF development more than sulphate content. In this paper, we investigate the ability of mortars made of 100% recycled sand to develop DEF damage when cured at early elevated temperatures and to compare them to mortars made of natural siliceous sand that are known from past studies to develop DEF. [6,12,30,31].

Table 1 – Maximum substitution percentages of RCA aggregates according to the European standard [NF EN 206/CN, 2014]

RCA aggregate type	Exposition classes			
	X0	XC1 ; XC2	XC3, XC4, XF1, XD1, XS1	Other exposition environments
Type 1 RCA gravel	60	30	20	0
Type 2 RCA gravel	40	15	0	0
Type 3 RCA gravel	30	5	0	0
RCA sand	30	0	0	0

2. Experimental study

Ten mortars were studied for delayed ettringite formation. Three mortars formulations were added sodium sulphate to enhance ettringite formation. Adding sodium sulphate is commonly used in DEF studies to amplify DEF effects [15–17,32]. Three formulations were made without any additions, four remaining formulations used blended RCA sand with gypsum plaster powder to simulate sulphate pollution. Mortars were cured according to a four-stage heat treatment reaching a maximum temperature of 80°C which is the same four-stage heat treatment used by Nguyen et al [16,33], Amine et al. [15] and similar to that used by Brunetaud et al. [34]. After curing, mortars were conserved in polypropylene plastic container filled with renewed demineralized water at 20°C.

2.1. Materials

2.1.1. Cement

The cement used in this study is a CEM I 52.5 N CE CP2 NF. Cement mineralogical and chemical composition is detailed in Table 2 and Table 3 respectively.

Table 2 − Mineralogical composition of the cement used in mortar formulations

Compound	Mass
C_3S (%)	63
C_2S (%)	14
C_3A (%)	9
C_4AF (%)	9
Density (g/cm^3)	3.16
Specific surface Blaine SSB (cm^2/g)	3829

Table 3 − Cement chemical composition

Compound	Na_2O eq.	SO_3	Cl^-	S^{2-}	loss on ignition	Insoluble residuals
Content (% by weight of cement)	0.8	3.1	0.05	0.01	1.2	0.5

2.1.2. CEN-Standard Sand

CEN-Standard Sand is used in two mortar formulations. The sand meets the standard NF EN 196-1 [35] specifications, it is classified as non-alkali silica reactive according to the standard NF P18-594:2015 [36].

2.1.3. Recycled sand screening and preparation

Recycled aggregates were provided by two CDW (concrete and demolition waste) platforms. The first platform is located in western France in Quimper city. The second platform is located near Paris for a company specialised in recycled and natural aggregates. Aggregates were delivered in big bags. The original grain size cut was 0/20 mm for Quimper aggregate and 0/6 mm for Paris aggregate. Screening was used to obtain 0/2 mm grain size cut for both RCS (recycled concrete sands) which corresponds to the reference siliceous sand grain cut size. Granular reconstitution was done to obtain similar RCS particle size distribution with 5% of fine particles ratio. Figure 1 shows the particle size distribution for the standardised sand and for both RCA sands: Quimper recycled sand noted « RCS-Qpr » and Paris sand noted « RCS-Prs ».

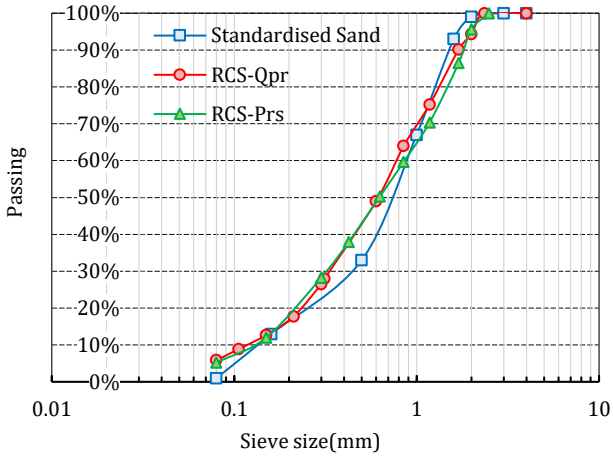

Figure 1 – Particle size distribution for the standardised sand and for the two reconstituted recycled sands RCS-Qpr and RCS-Prs.

Absorption and density were determined according to the standard NF EN 1097-6 [37] while sulphate and water-soluble alkaline content were determined according to NF EN 1744-1 and LPC N°37 standards respectively [26,38]. Table 4 summarizes the results of the analyses described. Sand pore size distribution was measured by mercury intrusion porosimetry using 2.5 grams of each recycled sand, results are shown in Figure 2. X-ray fluorescence spectrometry (XRF) was done on recycled sands, the chemical constitution of the RCS is detailed in Table 5. The contents of the main elements reflect the regional particularities of the aggregates used in concrete manufacture.

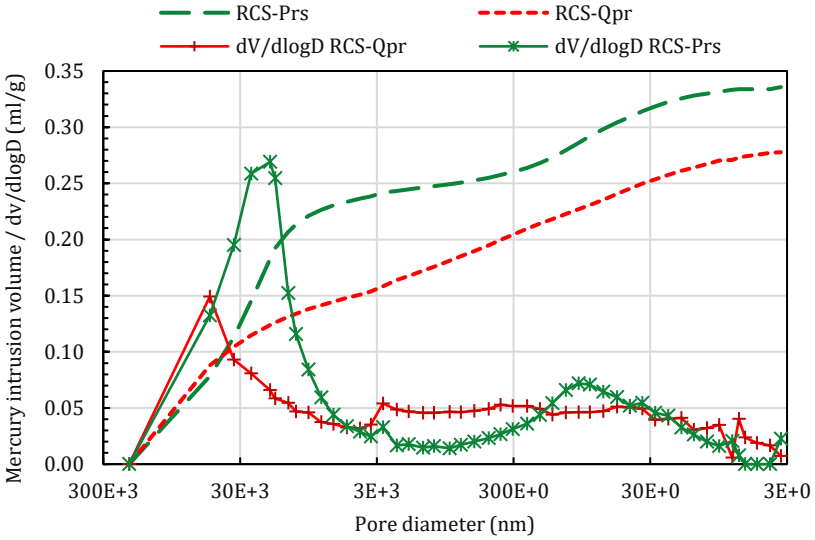

Figure 2 – Pore size distribution in Quimper and Paris sands.

Table 4 – Apparent density, absorption, sulphate and alkaline content for Quimper and Paris RCS.

Recycled sand	Apparent density (kg/m³)	Absorption (%)	Sulphate content (% SO_4^{2-} bwa)	Water soluble Na_2O eq. (mg/kg)
RCS-Qpr	1915	14.5	0.21	1300
RCS-Prs	2100	10.0	0.29	686

Table 5 – X-ray fluorescence analysis results.

Compound (% bwa)	RCS-Qpr	RCS-Prs
Na_2O	0.83	0.18
MgO	0.46	0.67
Al_2O_3	8.24	2.72
SiO_2	61.26	52.83
P_2O_5	0.13	0.06
SO_3	0.65	0.54
K_2O	2.32	0.56
CaO	11.37	21.66
TiO_2	0.18	0.11
MnO	0.04	0.04
F_2O_3	1.38	1.02
SrO	0.01	0.03
loss on ignition	12.83	19.40
Total	99.70	99.82

Both aggregates are rich in silica with RCS-Qpr having a higher amount (61%) than RCS-Qpr (52%). Calcium oxide constitute 21.7% of RCS-Prs while it constitutes 11.4% of RCS-Qpr, alumina (Al_2O_3) is more present in RCS-Qpr (8.2% versus 2.7%). According to the results, RCS-Qpr is rich in quartz and anorthite feldspar which reflects the geological nature of the French Britany region. On the other hand, RCS-Prs is half quartz and a third limestone (22% CaO with the molar ratio ($CaCO_3$/CaO) = 1.78).

2.1.4. Sulphate pollutions and additions

Gypsum plaster was used to simulate sulphate pollution in recycled aggregates. Plasterboards were made and dried at 50°C for 48 hours. A steel mortar and a pestle were used to crush the plasterboard after the plaster panels were broken into small pieces. Two sieve of 2 mm and 100 µm were used to obtain two different grain size cuts, less than 100 µm and 100 µm-2mm. Both obtained plaster powders were analysed for water-soluble sulphate content. The plaster powder with a fineness of less than 100 µm had a soluble sulphate content of 49.7% and that of [0.1-2] mm cut had a soluble sulphate content of 47.5%. Both sulphate contents are slightly lower than the theoretical sulphate content of calcium sulphate dihydrate (~55.8%) which is the major constituent of gypsum plaster. Sodium sulphate was used in three formulations to enhance ettringite formation. The product used is a chemical lab-grade Na_2SO_4 powder with a minimum purity of 99%.

2.2. Preparation and conservation

2.2.1. Mixing procedure and thermal curing

Ten mortar formulations were done using the three sands (standard sand, RCS-Qpr and RCS-Prs). All the formulations respect the following ratios by weight, water-to-cement ratio = 0.5; sand-to-cement ratio = 3 or (sand + plaster powder)-to-cement ratio = 3 except the "Prs-SS" formulation which is done with w/c=0.55 due to a workability problem during casting. Changing the water-to-cement ratio in "Prs-SS" from 0.5 to 0.55 will result in higher porosity, lower density and impact DEF symptoms due to change in microstructure. This impact is likely to be minor; it is taken into consideration in results analysis. Three formulas "Ref-SS", "Qpr-SS" and "Prs-SS" were made using sodium sulphate addition to reach 5% content of sulphur trioxide by weight of cement. Sodium sulphate was dissolved in the mixing water before adding it to the cement and sand. Three other formulas were done using the RCS without any addition ("Ref", "Qpr" and "Prs"), other last four formulations were done using blended RCS with plaster powder. The sulphate polluted sand is obtained by replacing in the recycled sand the exact amount of plaster powder needed to obtain a soluble sulphate content of 1.2% or 0.8%. "Qpr-1.2CP" and "Qpr-1.2FP" formulations are made from Quimper recycled sand with 1.2% bwa of soluble sulphate using [0.1-2] mm and 0.1 mm fineness

respectively. “Prs-1.2FP” is made from Paris recycled sand with 1.2% bwa of soluble sulphate using 0.1 mm fineness. “Qpr-0.8FP” is made from Quimper recycled sand with 0.8% bwa of soluble sulphate using 0.1 mm fineness. Table 6 summarizes the composition of each formulation.

Table 6 − Mortar formulations.

Class	Code	Sand type (g)			Na_2SO_4 (g)	Plaster powder type (g)	
		CEN Stand. Sand	RCS-Qpr	RCS-Prs		Fine plaster <0.1 mm	Coarse plaster [0.1 − 2] mm
Sodium sulphate added	Ref-SS	1350			13.5		
	Qpr-SS		1350		13.5		
	Prs-SS			1350	13.5		
Without additions	Ref	1350					
	Qpr		1350				
	Prs			1350			
Gypsum powder polluted	Qpr-1.2CP		1322				28.1
	Qpr-1.2FP		1323			27.0	
	Qpr-0.8FP		1334			16.1	
	Prs-1.2FP			1325		24.8	

Mortars were casted in prismatic stainless-steel moulds (ref. E0107; L0722-E0104/01) having the dimensions of 40×40×160 mm^3 and in cylindrical moulds having the dimensions (D = 65 cm; H = 130 mm) and (D = 110 mm; H = 220 mm). Three prismatic moulds for each formulation were equipped with upper and lower studs for expansion measurement. Cylindrical samples were used for permeability tests only. Casting procedure was done according to NF EN 196-1 [35] standard in the case of natural sands formulations. RCS mortars preparation was adjusted to take into consideration workability difficulties, as it was noticed that RCS mortars takes more time to be well mixed. RCS sands were moistened 24 h in advance to mixing by the quantity of water equal to their absorption plus 5% of the mixing water [39]. The cement was mixed with the moistened RCS for 1 minute at medium speed, then the mixing water is added and mixed at high speed for 1 minute and a half, then the mixer is stopped and the bottom was scrapped, finally, the mixing was resumed for 2 minutes. The casting was done same as per NF EN 196-1 standard. Heat curing program was the same as DEF studies of Amine et al. [15], Nguyen et al [16] and very close to that used by Martin et al. [40] and Brunetaud et al. [34]. The first stage of the thermal cure consists of protecting casted moulds by a plastic film to limit evaporation and keep them in a temperature-controlled room at 20°C for 2 hours. The mortars are then placed in the oven to start the second stage. The temperature is then increased linearly for 22h to 80 °C (second stage) and maintained constant for 72 h (third stage) and finally decreased to reach 20 °C during 55 h (fourth stage).Type K thermocouples were placed in the oven and at the core of one sample, temperature was recorded every 15 min. Figure 3 shows the setpoint and both recorded temperatures from the second to the fourth stage. The temperatures of the oven and at the core of the sample follow exactly the set temperature curve. However, at the end of the thermal cycle, the temperature of the oven and sample decreases slowly, which is explained by the decreasing heat exchange capacity at smaller temperature difference between the oven and the ambient air.

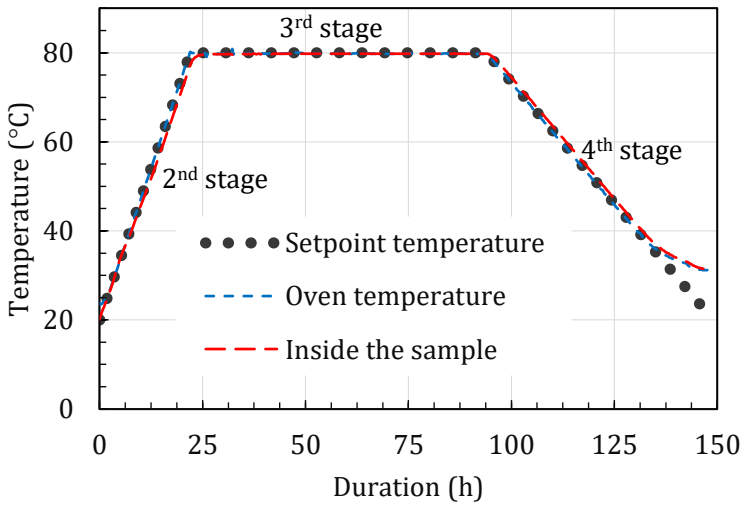

Figure 3 – Temperature evolution during the thermal cure

The samples were removed from the moulds and stored in closed polypropylene plastic storage boxes filled with deionized water at 20 °C. Filled water volume was equal to 130% of mortar samples volume to limit excessive lixiviation of calcium hydroxide. Water was renewed at once every 3 days during the first two weeks, and later once every two weeks for 2 months and finally once every two months until the end of the testing period.

2.2.2. Fresh mortar tests

Mortar workability was tested immediately after mortar mixing using a workability meter « LCL » (ref. C0209/1) formed by a steel parallelepipedal mould equipped with a vibrator. The mould is divided into two partitions separated by a removable steel wall. The test consists in measuring the time T of flow of a given fresh mortar under the vibration according to NF P 18-452 [41] standard. The second test was to weigh several moulds (≥3) before and after casting in order to compute fresh mortar density. Figure 4 shows mortar formulations flow time and mortar fresh density charts. Workability test was not done for the two formulations Ref-SS and Qpr-SS. The workability of "Ref-SS" and "Qpr-SS" formulations is likely to be close to that of "Ref" and "Qpr" respectively. An important increase of flow time is noticed when plaster powder is added to Quimper mortars. This decrease in workability could be caused by microstructural changes and chemical interactions between recycled sand and gypsum particles. Moreover this phenomenon did not appear in mortars made of Paris sands. Probably there is a specific interaction between Quimper sand and gypsum but no other tests were able to identify the exact origin behind this phenomenon. Reference mortar fresh density (~2200 kg/m^3) is largely higher than RCA based mortar. Mortars made of Paris sand have slightly greater fresh density (1904 - 1980 kg/m3) than Quimper sand based mortars (1870 – 1895 kg/m3). Paris sand have lower porosity and higher density comparing to Quimper sand for this reason their mortars are denser.

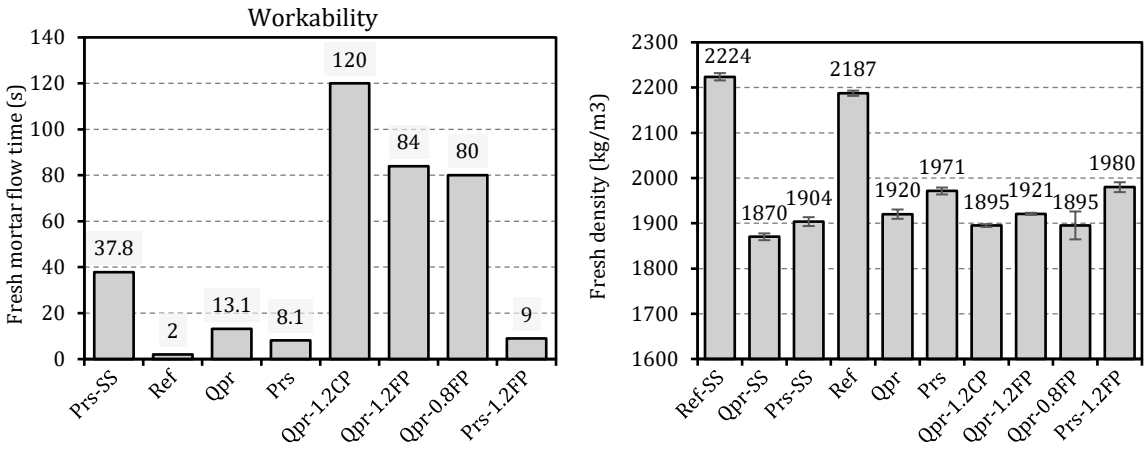

Figure 4 – Mortar workability flow time and fresh density

2.3. Samples monitoring and testing

Three mortars of each formulation were measured for expansion, mass uptake and dynamic Young modulus. Axial expansion was monitored using an extensometer with a resolution of ±1μm that measures length variation using the fixed studs on the top and the bottom of the prism (see Figure 5). Mass was measured using a digital scale with a resolution of ±0.1 g, while dynamic Young modulus was measured by a non-destructive impulse excitation technique using the Grindosonic® device. The sample is excited into vibration through the means of a light tap while a small vibration sensor in contact with the sample sends the signal to the device which displays the frequency. The dynamic Young modulus is then determined using the dimensions of the sample and its weight according to the standards ASTM E1876 – 15 and NF EN ISO 12680-1 [42,43].

Figure 5 – Measuring axial expansion with the extensometer.

Compressive and tensile strength were determined according to the European standard NF EN 196-1. Each tensile result consists in the mean strength of the three-point bending test on three samples at 28 days, 90 days and 180 days of immersion in water and the mean strength of four samples at 360 days. Submitted prisms to the three-point bending test are broken into two half-prisms which are both tested to compressive resistance; thus, each sample is submitted to one three-point bending test and 2 compressive tests.

Porosity and apparent density tests were done according to NF P 18-459 standard [44] which consists in measuring the buoyant mass of the saturated specimen in water, the saturated surface-dry mass and the

oven-dry mass at 105°C. Porosity is then computed using three measured values. Moreover, pore size distribution was measured by mercury intrusion porosimetry (MIP). Samples had a volume of 2 to 5 cm^3 and weighed between 3 and 10 g, they were sawn from prismatic cores and dried in an oven at 40°C for at least two weeks until mass stabilization. The MIP apparatus used was the AutoPore IV 9500 which can intrude pressure up to 400 MPa. The mercury contact angle taken into the pore size computation was 130° and the surface tension was 0.485N/m.

Gas permeability was measured on two samples at each deadline except on some deadlines when one sample was available only. Specimens were cylinders of 50 mm thickness and 65 or 110 mm of diameter. Under three to five different pressures (P_i [Pa]) are applied until a steady flow of nitrogen gas is measured on the output of a specimen at atmospheric pressure (P_{atm} [Pa]). Apparent permeability (K_A [m^2]) is then computed at each absolute injection pressure (Pi [Pa]) [45]. The intrinsic permeability (K_v [m^2]) is obtained by plotting K_A at different pressures against the inverse of the mean pressure $1/P_m=2/(P_i+P_{atm})$ and finding the value at the intersection of the straight trendline of the points with the vertical axis. The Klinkenberg coefficient is obtained by dividing the slope of the trendline by K_v.

SEM (Scanning Electron Microscopy) analysis was done using ZEISS EVO®4 electron microscope equipped with a secondary electron sensor and a backscattered electrons sensor. Prismatic sample cores were sliced and polished at different ages into square shapes of 2cm×2cm by 0.5 cm thickness. A gold coat was deposited on the surface which enables to use the High-Vacuum (HV) mode [46,47]. Analysis was focused on ettringite crystallization, microstructural changes and mineral composition using EDS (Energy Dispersive X-Ray Spectroscopy).

3. Results

3.1. Effect of sodium sulphate addition

3.1.1. Expansion, mass uptake and dynamic modulus evolution

Sodium sulphate addition is expected to enhance delayed ettringite formation [32] as it constitutes an excellent soluble sulphate compound. Expansion curves for mortar formulations with and without sodium sulphate are shown in Figure 6. An expansion exceeding 0.04% is considered as a positive indicator for DEF damage [48]. “Ref-SS” and “Qpr-SS” mortars exhibit DEF related expansion and reached the DEF indicator of 0.04% expansion at 90 days and 28 days respectively. The reaction started faster in the Quimper based mortar as compared to the standardised based mortar. After one year of immersion in water, expansion reached a maximum of 0.95% and 0.1% for “Ref-SS” and “Qpr-SS” respectively. “Prs-SS” and the three mortars without additions show very little expansion after one year of conservation. A maximum expansion of 0.04% is measured for “Qpr”, “Prs-SS” and “Prs”; 0.02% for “Ref” mortar. Sodium sulphate addition in “Prs-SS” did not induce higher expansion as opposed to the Quimper and the reference sand formulations.

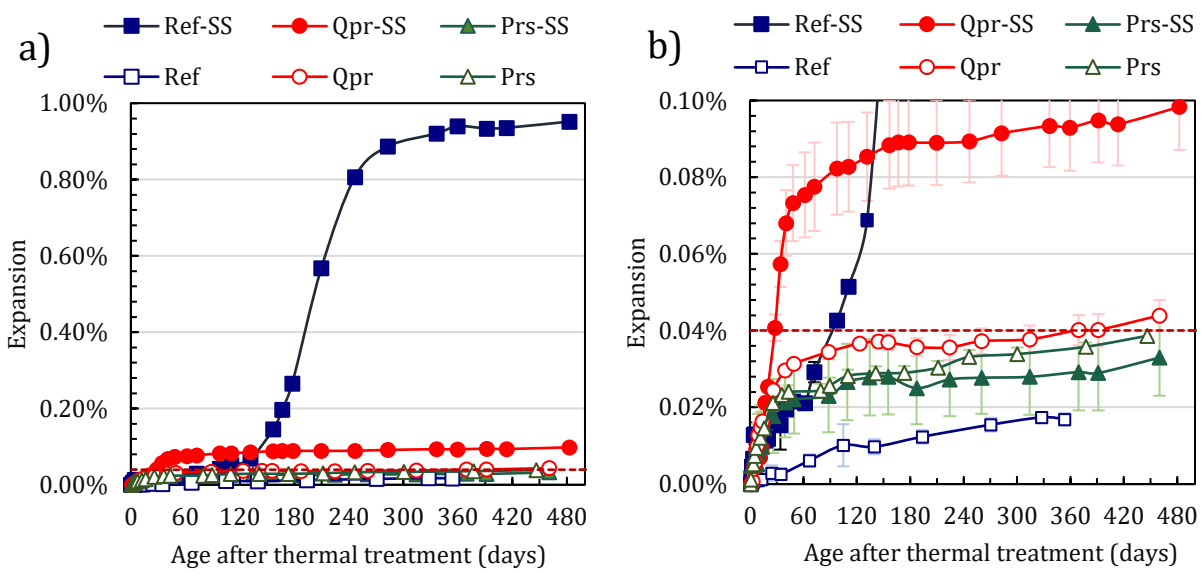

Figure 6 – Expansion of the 6 formulations "Ref-SS", "Ref", "Qpr-SS", "Qpr", "Prs-SS" and "Prs". Both graphs a) and b) represents the same curves with two different scales on Y axis.

Figure 7 shows the evolution of mass uptake which is known to increase with DEF expansion due to microcracking development and absorbed water needed for ettringite formation [15,16,49]. Reference mortars show similar mass uptake until the moment when "Ref-SS" started expanding (120 ~ 280 days). A sigmoid mass uptake curve is seen in "Ref-SS" mortar while "Ref" didn't show any modification in mass evolution which keep going up slowly. Recycled sand based mortars mass did not exhibit any sigmoid mass uptake, their mass increased drastically from the beginning and continued increasing at a lower rate with time. Both recycled sand based mortars with sodium sulphate reached 4.5% of mass uptake at 1 year while sodium sulphate free mortars increased 3% in this period. The difference in mass uptake is mostly seen at the beginning for mortars made of recycled sand which is accompanied with the early expansion of "Qpr-SS" during the first month. This concomitance of early mass uptaking and expansion in case of "Qpr-SS" could be a consequence of a quick ettringite crystallization that did not lead to a large amplitude of expansion. Concerning the mass uptake of "Qpr" and "Prs", there is no doubt that the majority of absorbed water is not the consequence of DEF and it may be a sign of a hydration process which has been retarded by the elevated absorption and porosity of RCS and the curing cycle.

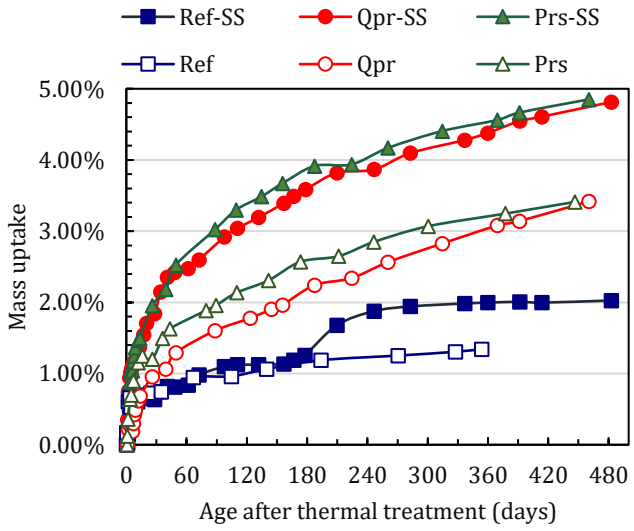

Figure 7 – Mass uptake of the 6 formulations Ref-SS, Ref, Qpr-SS, Qpr, Prs-SS and Prs.

Regarding the dynamic Young modulus (Edyn), Figure 8 shows the evolution of Edyn, while Figure 9 shows the dynamic modulus variation from its value at the first day of immersion in water which is detailed in equation [1]. The dynamic modulus increases with time for all mortars and at a higher amount in RCS mortars, which is a second clue of an ongoing hydration. "Ref-SS" started losing its stiffness at 120 days when expansion kicked up and continued till 270 days with a 40% loss in stiffness. After 270 days the stiffness started going back up and recovered partially till 480 days. Furthermore, the dynamic modulus gain increased more in "Qpr-SS" than "Qpr" mortars while the opposite is seen in "Prs-SS" and "Prs" mortars. This difference could be attributed to the difference in cement to water ratio which is equal to 0.55 in "Prs" mortar while other mortars have a ratio of 0.5. A correlation between Young modulus loss and expansion was done on "Ref-SS", pozzolan and fly ash added mortars formulations [16,50,51]. A comparison was done between the experimental results and a poromechanical model [51] where Young's modulus decrease as a function of the overall expansion in the same way as the experimental results.

$$\Delta E_{dyn} = \frac{E_{dyn} - E_{dyn}(1^{st}\ \text{day})}{E_{dyn}(1^{st}\ \text{day})} = \frac{E_{dyn}}{E_{dyn}(1^{st}\ \text{day})} - 1 \qquad [1]$$

[Insert Figure 8 here] [Insert Figure 9 here]

3.1.2. Porosity and pore size distribution evolution

Porosity testing is done at 28, 90, 180 and 360 days of immersion in water. The evolution of mortar porosity and apparent mortar density is given in Figure 10. Regarding the age of testing, porosity seems to be largely higher in mortars made of recycled sand than standardised sand. The highest porosity is found in Quimper based sand mortars about 35 to 37.5 % at 28 days. Paris sand based mortars porosity at 28 days is about 30 to 31 % while the porosity for the standardised based mortars is 18 to 20 %. Unlike the standardised sand, recycled sands particles are highly porous and their porosity is mostly provided by their paste. Thereby, higher paste content is linked to higher absorption which is the case of Quimper sand whose absorption is equal to 14.5% comparing to 10% for Paris sand (see Table 4). Additionally, the evolution of mortar porosity seems to increase in RCS-mortars till 180 days and decreases a little after. A possible explanation could be that hydrate content increases with age, and subsequent drying at 105°C partially dehydrate them, which increases artificially the measured porosity. Although this may be true, Yacoub et al. found that the difference of RCS mortar porosity between 60°C and 105°C is the result of the capacity of RCS to stock water at higher temperatures far below natural aggregates (till 80°C) and not of their paste dehydration [52].

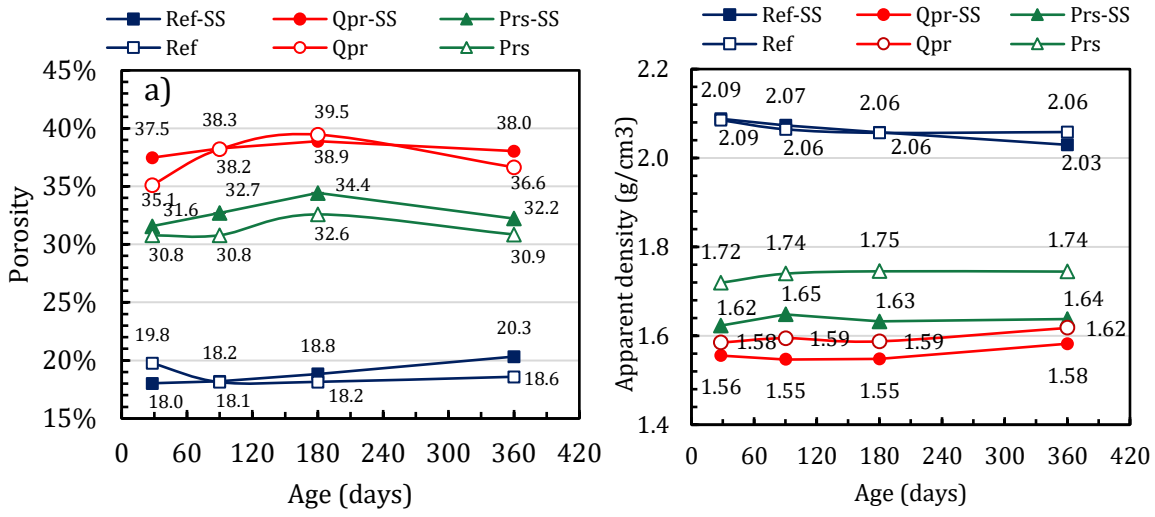

Figure 8– Porosity (a) and apparent density (b) evolution for the mortars Ref-SS, Ref, Qpr-SS, Qpr, Prs-SS and Prs.

There is a second more reasonable point that explains porosity evolution, based on water accessibility to the pores. The increase in mass uptake of RCS mortars shown in Figure 7 could have a second origin in addition to hydration, which could be potentially a continuous slow diffusion of water inside the paste in small pores that are abundantly present in RCS mortars (see Figure 12). The variation in porosity could be

the result of the inability to fully saturate all pores during the vacuum absorption phase. The indicator that could validate this hypothesis is the skeletal density (SD) shown in Figure 11. Porosity is expressed as a function of the apparent density (AD) and the skeletal density (SD) in equation [2]. According to the equation, the skeletal density and the porosity vary similarly as long as AD is constant.

$$\text{Porosity} = 1 - \frac{\text{AD}}{\text{SD}} \qquad [2]$$

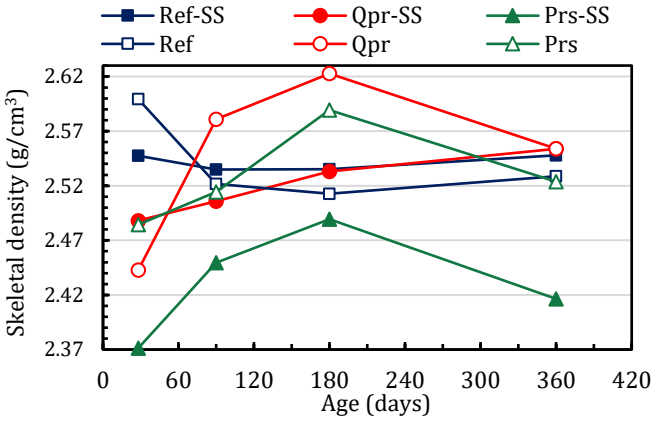

Figure 9– Skeletal density evolution for the mortars Ref-SS, Ref, Qpr-SS, Qpr, Prs-SS and Prs.

The skeletal density of "Qpr", "Prs-SS" and "Prs" mortars shows similar positive increment between 28 days and 180 days, and it decreases between 180 and 360 days. Mortar porosity evolved in the same way as skeletal density while the apparent density shows little or no evolution. At the age of one year "Qpr", "Prs-SS" and "Prs" mortars were kept at 20°C and 50% humidity for two weeks before the porosity test. The drying condition of the samples was shorter for the first deadlines (28, 90 and 180 days), not more than 4 days. Thus, potentially during the drying phase, a big part of water was pulled out from the pores and was not filled later during the porosity test. This difference in testing conditions could be the origin of the drop in the porosity results. To correct this problem, the skeletal density can be estimated at 180 days and the porosity will be obtained according to the variation of the apparent density from equation [2]. In that case, RCS-mortars porosity will show no important variations, only "Ref-SS" mortar porosity will show a positive evolution. Consequently, the porosity results are difficult to interpret without additional tests, nonetheless the damaged mortar "Ref-SS" showed a significant increase in porosity which is mostly the result of DEF induced microcracking due to expansion.

To see more precisely the characteristics of the porous medium, mercury intrusion porosimetry (MIP) was measured at the age of 1, 3, 6 and 12 months for "Ref-SS" and "Qpr-SS" mortars, while the remaining mortars were measured at 1 month and 6 months age. Only the results of one month and six months are presented in Figure 12 as they sufficiently represent the evolution of the porous distribution. Furthermore, adding the 3-month and 1-year curves complicates reading the graphs while providing little additional information. Pore size distribution changes from 28 days to 180 days in a similar way for all mortars except for "Ref". Medium size pores volume (30-300 nm) decreases while small size pores volume (< 30 nm) increases. Unlike the majority, "Ref" mortar did not show any displacement in pore size distribution, on the contrary, it shows an increase in porosity. Total intrusion volume decreases for "Ref-SS" from 0.07 ml/g to 0.062 ml/g while it increases for "Ref" mortar from 0.06 ml/g to 0.075 ml/g. The evolution in pore size distribution could be the result of ettringite crystallization. Ettringite starts appearing first in heat-cured cementitious materials in C-S-H surrounding pores which are nanometric. Over time, ettringite crystals start to dissolve and to migrate through ions diffusion toward larger pores [53]. Based on pore size distribution results, adding sodium sulphate seems to amplify the displacement in the pore size distribution, which is clear in the reference formulations and to a lesser extent in the recycled sand formulations. However, ettringite recrystallization is not the only phenomenon that modifies the pore diameter distribution, continuous hydration process of the remaining clinker is another phenomenon where large pores are filled by new C-S-H that fill available capillary pores with a new paste having smaller pores. The third phenomenon which changes the distribution of pore diameter is the development of microcracking, which produce openings in the range of [1-25 µm] largely greater than initial average pores diameter [20-50 nm]. This phenomenon

was seen on the porosity size distribution of damage mortars ("Ref-SS") after one year but is not shown here to limit graph congestion.

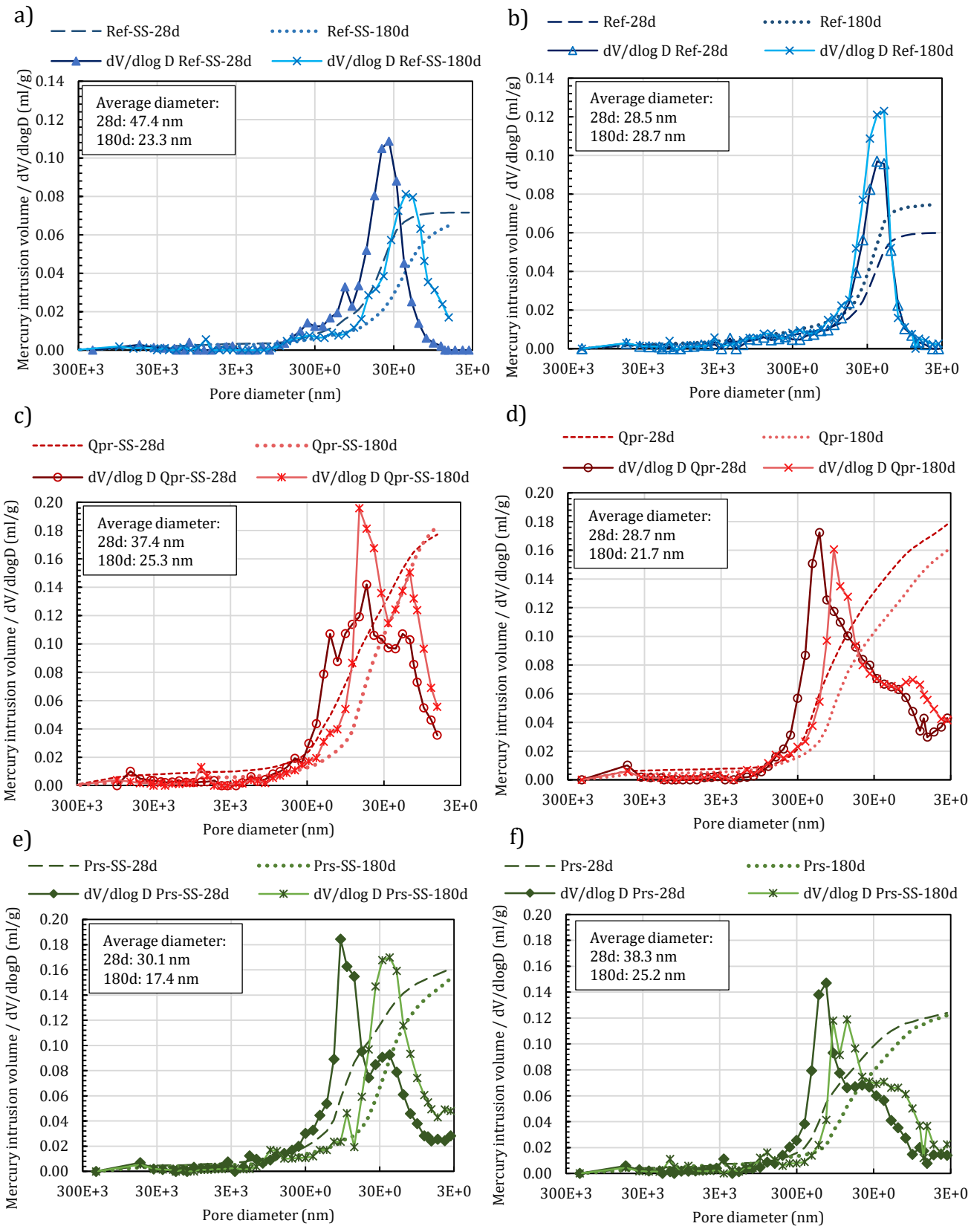

Figure 10– Pore size distribution for a) "Ref-SS", b) "Ref", c) "Qpr-SS", d) "Qpr", e) "Prs-SS" and f) "Prs" mortars at 28 and 180 days

3.1.3. Mortar compressive and tensile strength

Mortar compressive and tensile strength through 3-points bending test results are shown in Figure 13. "Ref-SS" and "Ref" mortars show the highest compressive strength starting 38 and 39 MPa respectively while both Quimper sand based mortars show the lowest compressive strength starting 16 MPa. "Prs-SS" mortar have a lower compressive strength than "Prs" for the reason that the formulation of "Prs-SS" has a higher water to cement ratio which is equal to 0.55 while it should be 0.5. The starting compressive strengths are 23 MPa for "Prs-SS" and 30MPa for "Prs". Higher porosity is found in "Prs-SS" in comparison to "Prs" according to porosity test and MIP test which proves that the lower strength of "Prs-SS" is the consequence of its higher w/c ratio. Regarding the evolution of the resistance, there is an increase in the compressive strength with time, which indicates a continuous hydration of the paste. Additionally, the decrease in the average pore diameter in all mortars shown in Figure 12 is a consequence of the continuous hydration process. "Ref-SS" mortar compressive strength decreased from 45.6 to 42.2 MPa between 90 and 180 days arising concomitantly with the start-up of expansion, mass uptake and the loss of stiffness. Although the mortar underwent a 0.9% expansion and a young modulus loss till 300 days, the compressive strength at 360 days went up back to 50.9 MPa. The increase in resistance can be explained by the capacity of ettringite to partially "repair" microcracking damage. Moreover, the microcracking plans do not appear to be in the direction of the shear stress, most plans are found to be parallel to the direction of the compressive force. This is attributed to the non-isotropic character of the expansion of prisms associated to their bending in a specific direction (see Figure 14). The "Prs" mortar shows a small decrease in compressive strength (33.2 to 31.7 MPa) between 90 and 180 days, which can be the result of samples heterogeneity, no other indicators reported any DEF damage.

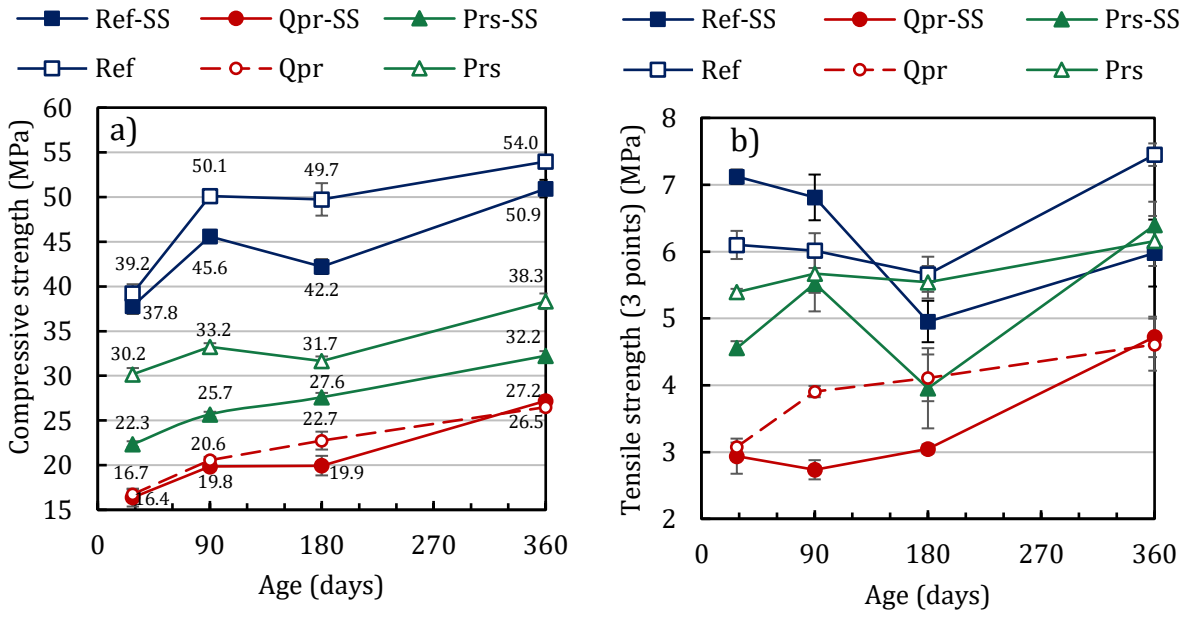

Figure 11– Mortar compressive (a) and tensile (b) strength evolution

The tensile strength of mortars increased with time except the DEF damaged mortar. "Ref-SS" mortar scores its highest strength of 7.1 MPa at 28 days, it decreases to 5 MPa at 180 days and went back up to 6 MPa at 360 days. The highest increase in tensile strength is for "Qpr-SS" and "Qpr" mortars which both register 3 MPa at 28 days and 4.6 MPa at 360 days. The remaining formulations exhibit variation in the tensile strength accompanied with an increase in the standard deviation of the results which can be attributed to the heterogeneity in samples. At 360 days all samples except "Ref-SS" scores higher tensile strength compared to their initial strengths at 28 days, the strength gain varies between +1 and +1.5 MPa.

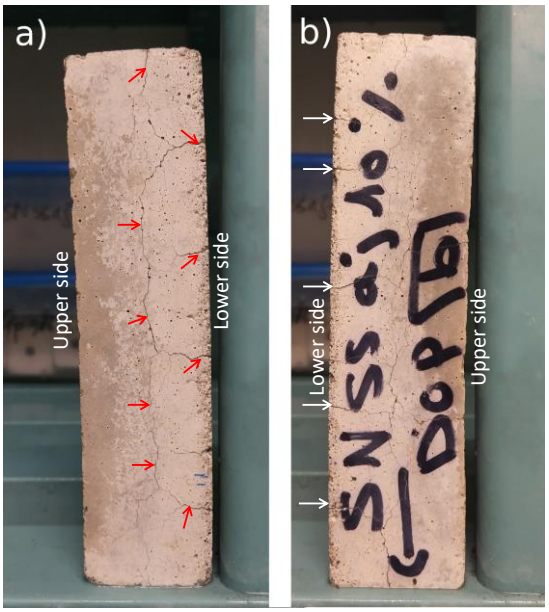

Figure 12– Two photos of the same sample "Ref-SS" showing the back (a) and the front (b) of the deformed prism (0.95% expansion at one year). The cracking appears on the lower side of the sample (the bottom side in the casting position) where it is visually noticed a more amplified expansion than that of the upper side.

3.1.4. Gas permeability

Gas permeability at 28,180 and 360 days was measured on all formulations and additionally at 90 days for "Ref-SS", "Ref" and "Qpr-SS" formulations. Figure 16 shows the apparent permeability of the mortars at 3 to 5 different mean pressures while Figure 15 shows the corresponding intrinsic permeability. Permeability is important in damage assessment as it is highly sensitive to microcracking [54].

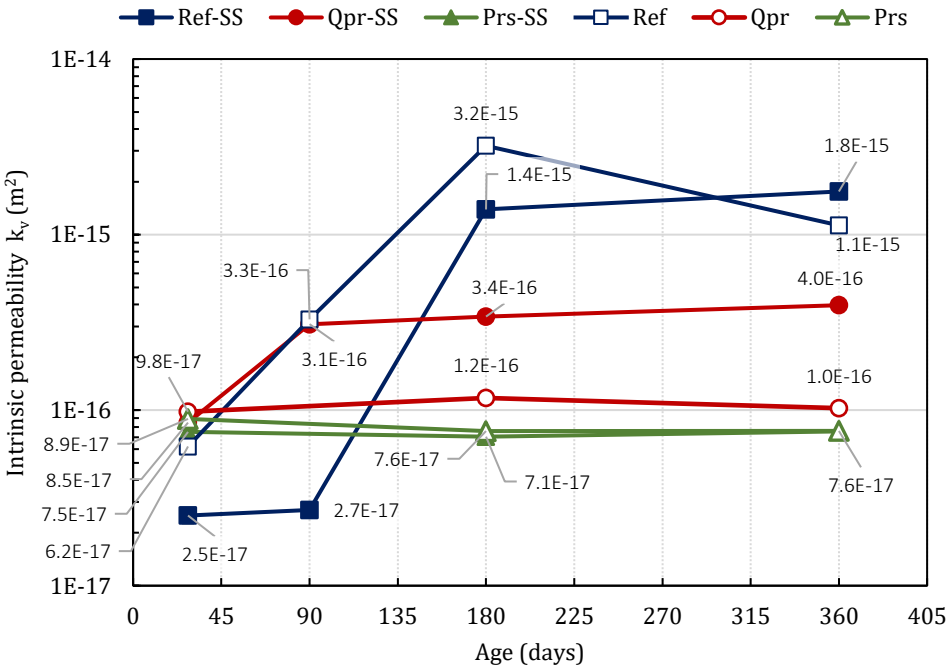

Figure 13– Evolution of the intrinsic permeability of the formulations "Ref-SS", "Ref", "Qpr-SS", "Qpr", "Prs-SS" and "Prs".

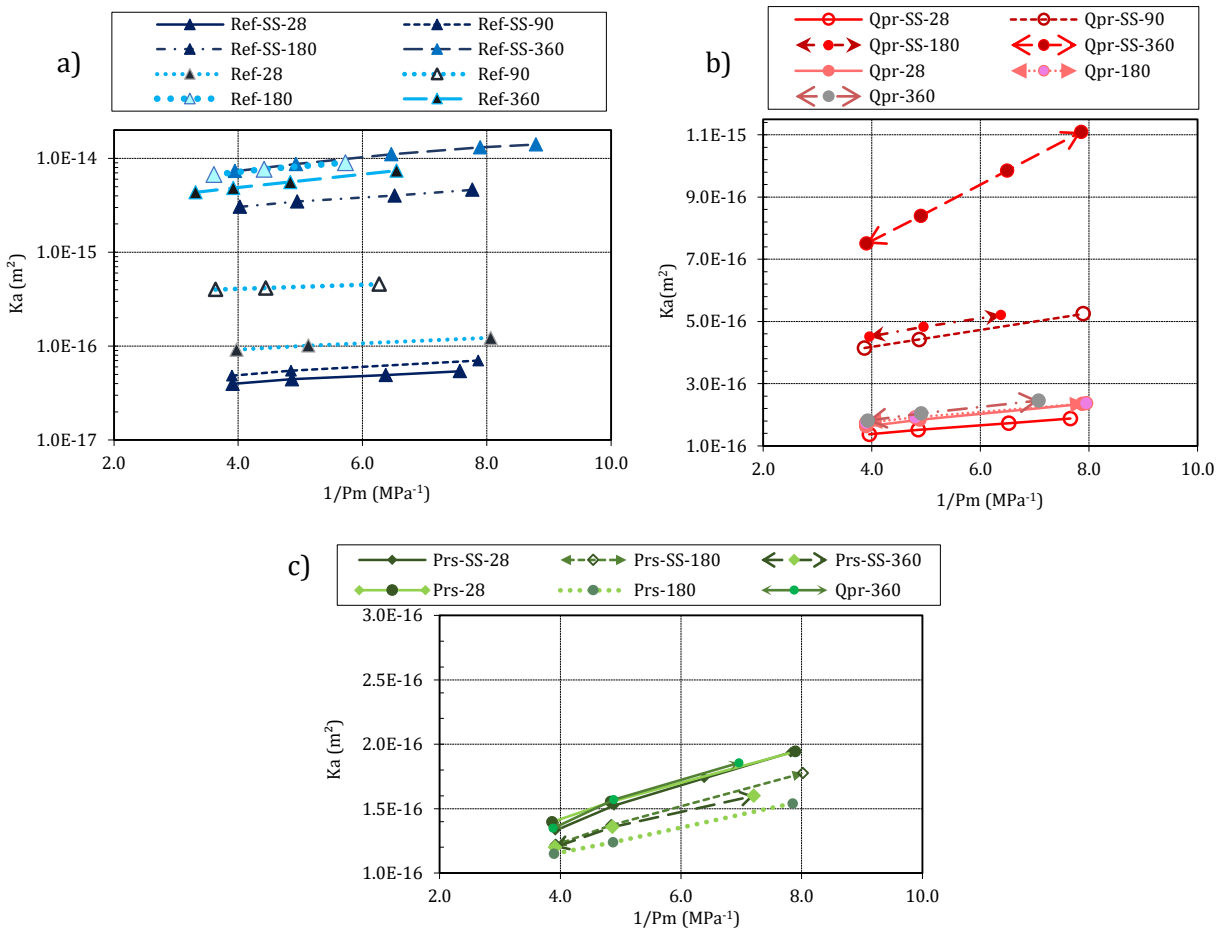

Figure 14– Apparent permeability at different ages for the mortars : "Ref-SS" (a) , "Ref" (a), "Qpr-SS" (b), "Qpr" (b), "Prs-SS" (c) and "Prs" (c).

"Ref-SS" and "Qpr-SS" mortars showed DEF related expansion in Figure 6, additionally they scored both significant permeability augmentation comparing to the mortars that had little expansion (<0.04%) except "Ref" mortar. The highest permeability increase is between 90 and 180 days for "Ref-SS" mortar (2.7×10^{-17} to $1.4 \times 10^{-15} m^2$) which corresponds to the period of the highest expansion gain and to the major loss in Young modulus. Equally, "Qpr-SS" mortars showed an enhancement in permeability between 28 and 90 days which corresponds to the period of their major expansion gain (see Figure 6), while no loss in the dynamic Young modulus has been noticed. However, "Ref" mortar scored an increase in permeability as high as "Ref-SS" mortar despite the absence of an expansion and of a loss in the dynamic Young's modulus. However, macro-cracking has been noticed visually on "Ref" cylinder samples which are used to measure permeability (Figure 17) while no cracks where noticed on the prisms. The difference between the samples could be attributed to the impact of the geometry on ions exchange and diffusion with the surrounding and inside the porous medium. Concerning the two Paris sand based mortars: "Prs-SS" and "Prs", none of them reported any enhancement in gas permeability and even a weak decrease is noticed.

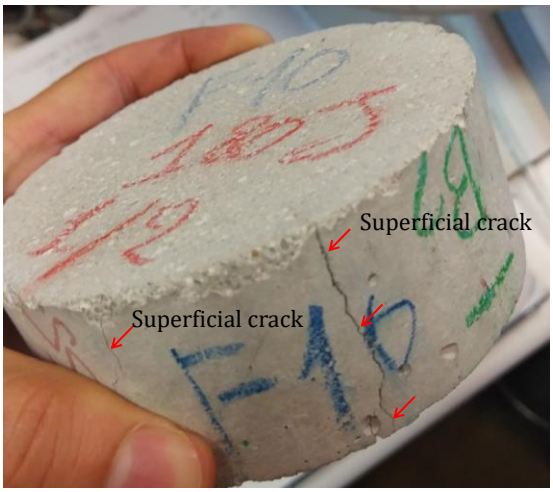

Figure 15– Photo of a mortar cylinder sample at 180 days ("Ref" formulation) showing macrocracks on the surface.

Figure 18 shows the correlation between the expansion and the permeability. Permeability is strongly correlated to expansion for low expansions. This correlation is shown for the two mortars "Ref-SS" and 'Qpr-SS". There is no increase in permeability for an expansion below 0.04% (DEF limit [48]) except for "Ref" mortar that presented cracking on permeability samples but not on prismatic samples that are used for expansion measurement. For high expansions the correlation between permeability and expansion decreases. It is possible that ettringite fills microcracks and modify permeability at large expansion when ettringite starts reaching large pores.

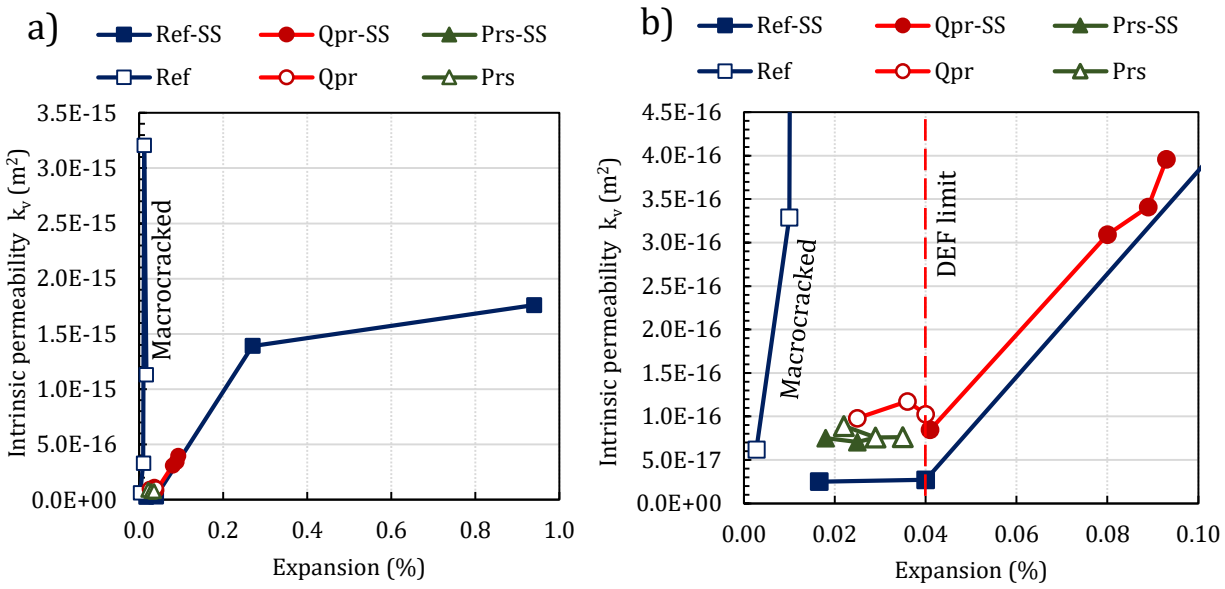

Figure 16– Graphic showing the correlation between expansion and permeability for the six mortars. Large expansions are shown in (a), whether fine expansions are shown in (b).

3.1.5. SEM observations

SEM was done at 360 days for all mortar samples and additionally at 90 days for sodium sulphate added formulations. SEM images can show microcracking, ettringite crystallization in paste, in microcracks and in the interfacial transition zone (ITZ). Figure 19 shows three SEM images for the sulphate added mortars at 90 days.

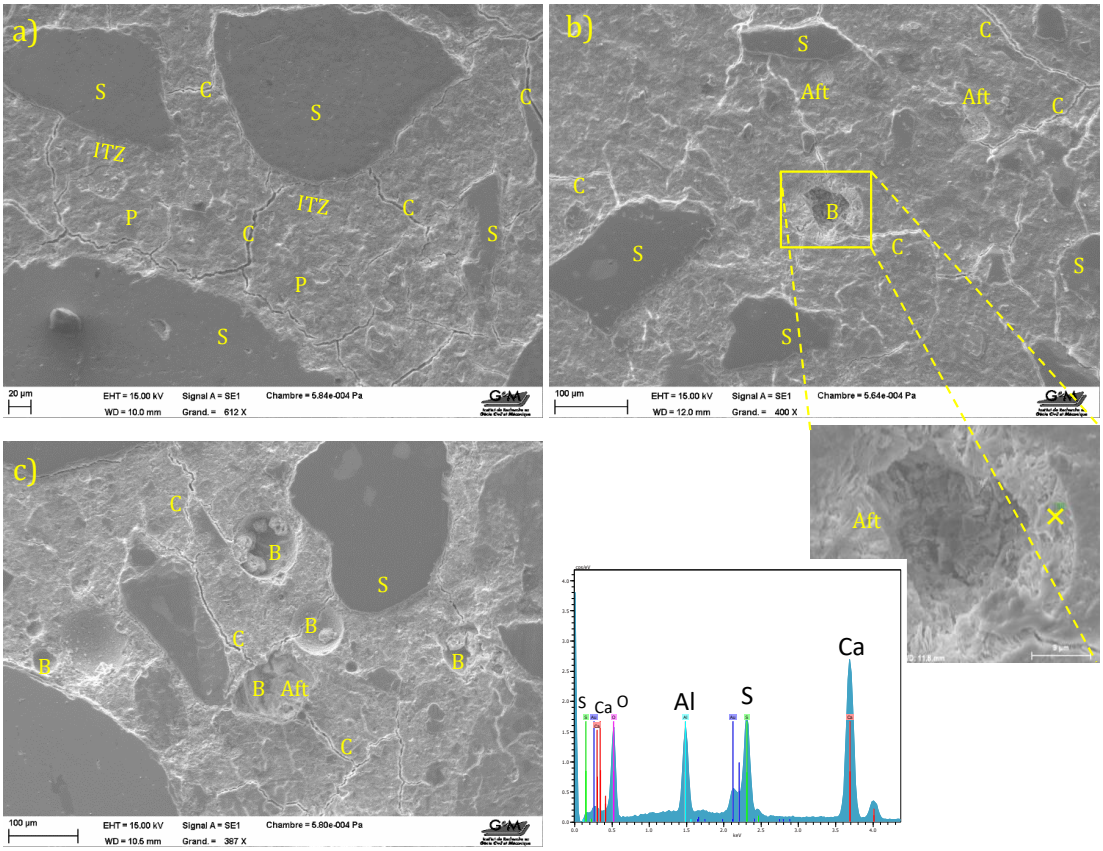

Figure 17– SEM images for "Ref-SS" (a), "Qpr-SS" (b) and "Prs-SS" (c) mortars at 90 days; expansion: 0.04% (a), 0.08% (b) and 0.02% (c). EDX spectrum shows ettringite crystals in air bubbles of "Qpr-SS" and to a lesser extent in "Prs-SS"; no Aft is detected in "Ref-SS". (P: Paste, S: Sand, C: Crack, Aft: Ettringite, B: Air Bubble).

The "Ref-SS" at 90 days had an expansion of 0.04% which is considered to be the onset of DEF damage. No visible ettringite was found and there was no debonding at the paste-aggregates interfaces. Some microckracking appears in the paste that could be mostly attributed to the shrinkage during the thermal curing, to the drying period after sample removal from water, or to sample sawing. Both "Qpr-SS" and "Prs-SS" show the presence of air bubbles in the paste having a diameter between 20 µm and 200 µm as a result of the elevated viscosity of fresh mortar mixtures made of recycled aggregates. Some air bubbles are filled partially with ettringite needle shaped crystals. Furthermore, at 360 days of age, "Ref-SS" mortar which scored an expansion of 0.95% shows ITZ debonding and ettringite filling the gap between the paste and the aggregates. Point 1 shown on the SEM image of Figure 20 is located at the ITZ which has a spectrum profile that corresponds to presence of aluminium, sulphur and calcium found in ettringite crystal. The point 2 located in the paste shows a massive ball of ettringite around five to ten µm of diameter. Massive ettringite balls of several micrometres are found almost everywhere in the paste of "Ref-SS" mortar at 360 days.

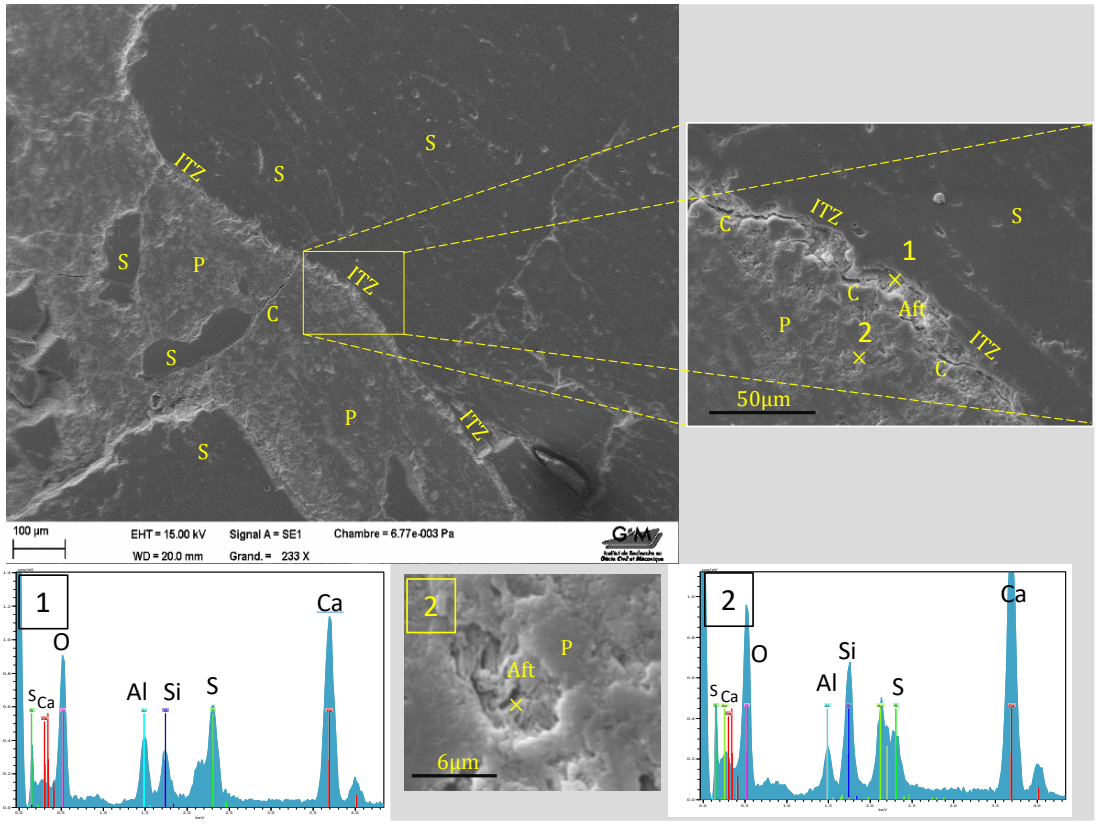

Figure 18– SEM image on "Ref-SS" sample at 360 days (0.95% expansion). Ettringite is detected by the EDX technique in the paste and in the interfacial transition zone (ITZ). (P: Paste, S: Sand, C: Crack, Aft: Ettringite).

Quimper and Paris sand based mortars with sodium sulphate shows large quantity of ettringite at 360 days filling the air bubbles. The expansion of "Qpr-SS" and "Prs-SS" reached 0.1% and 0.035% at one year of immersion in water, which is considered too small in comparison to the quantity of ettringite that is seen in the micrographs. Aluminate and sulphate ions migrated easily and found large volume in the entrained air to crystallize freely. Petrov found similar results using air entrainment in DEF susceptible concretes. It was shown that DEF expansion decreases when the volume of entrained air in the fresh concrete exceeded 2.8% [55]. For each 1% of entrained air volume that exceeds 2.8% there is a decrease of 0.25% in DEF expansion.

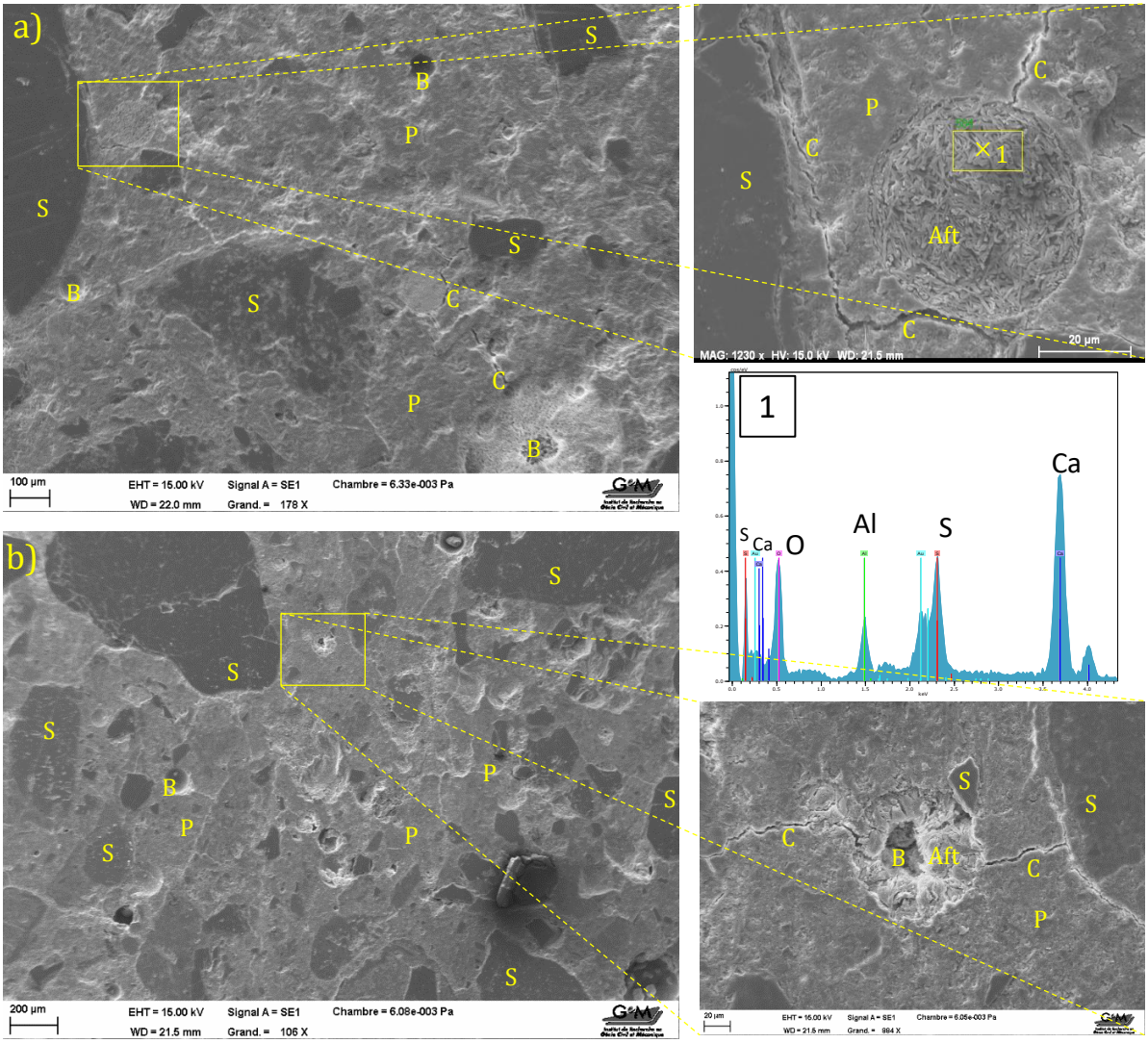

Figure 19– SEM image on "Qpr-SS" (a) and "Prs-SS" (b) samples at 360 days; expansion : 0.1% (a) and 0.03% (b). Ettringite crystallised in air bubbles mostly in "Qpr-SS". (P: Paste, S: Sand, C: Crack, Aft: Ettringite, B: air bubble).

The entrained air volume can be obtained by using the fresh mortar density and the mortar calculated density of the formulation using the formula:

$$\text{Air volume fraction (\%)} = 1 - \frac{\text{Calculated density}}{\text{Measured density}} \qquad [3]$$

The maximum expansion rate and the calculated entrained air for each mortar is shown in Figure 22. The correlation between the expansion and the entrained air is almost impossible to determine for the following reasons: the lack of variability of the expansions with a single elevated expansion and 8 almost equal expansions, the large variability of the factors influencing DEF other than the entrained air volume, such as the nature of aggregates, and the nature of additions. To establish a correlation, it is necessary to study the variation of one parameter and to fix the others whereas in our case the variability of the parameters is quite large compared to the number of formulations. Moreover, a difference of 3% to 7% of entrained air is calculated between mortars made of siliceous sands and the recycled sands. Assuming that the expected expansion for the mortars with recycled sand is equal to 1%, if the entrained air volume was below 2.8%, an addition of 4% (6.8% total) of entrained air will be able to decrease to zero the expansion of these mortars. Most of the studied mortars exceeds the 6.8% of entrained air volume which is the maximum limit not to exceed to obtain a significant expansion, therefore the studied mortars made of Quimper and Paris sands had little expansion. Furthermore, higher amount of sulphate and aluminate should be used to obtain significant expansions.

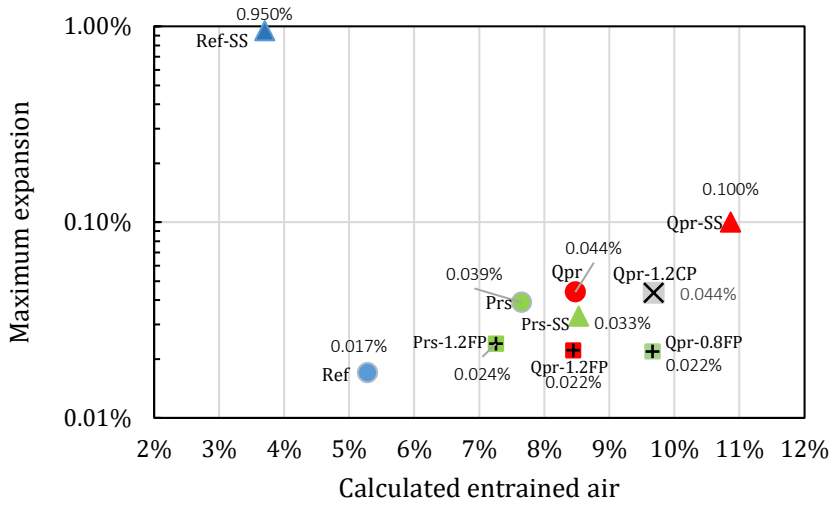

Figure 20– Graphic showing the maximum expansion rate of mortars and their calculated volume of entrained air.

Figure 23 shows the micrographs of "Qpr", "Prs" and "Ref" mortars at 360 days. Ettringite is found in all mortars in smaller quantities than in the formulations with sodium sulphate. The reference mortar "Ref" did not show any ITZ debonding which is coherent with a small expansion (<0.04%). Additionally, ettringite is not easily found in the reference mortar, however an ettringite ball was found (Figure 23 part d).

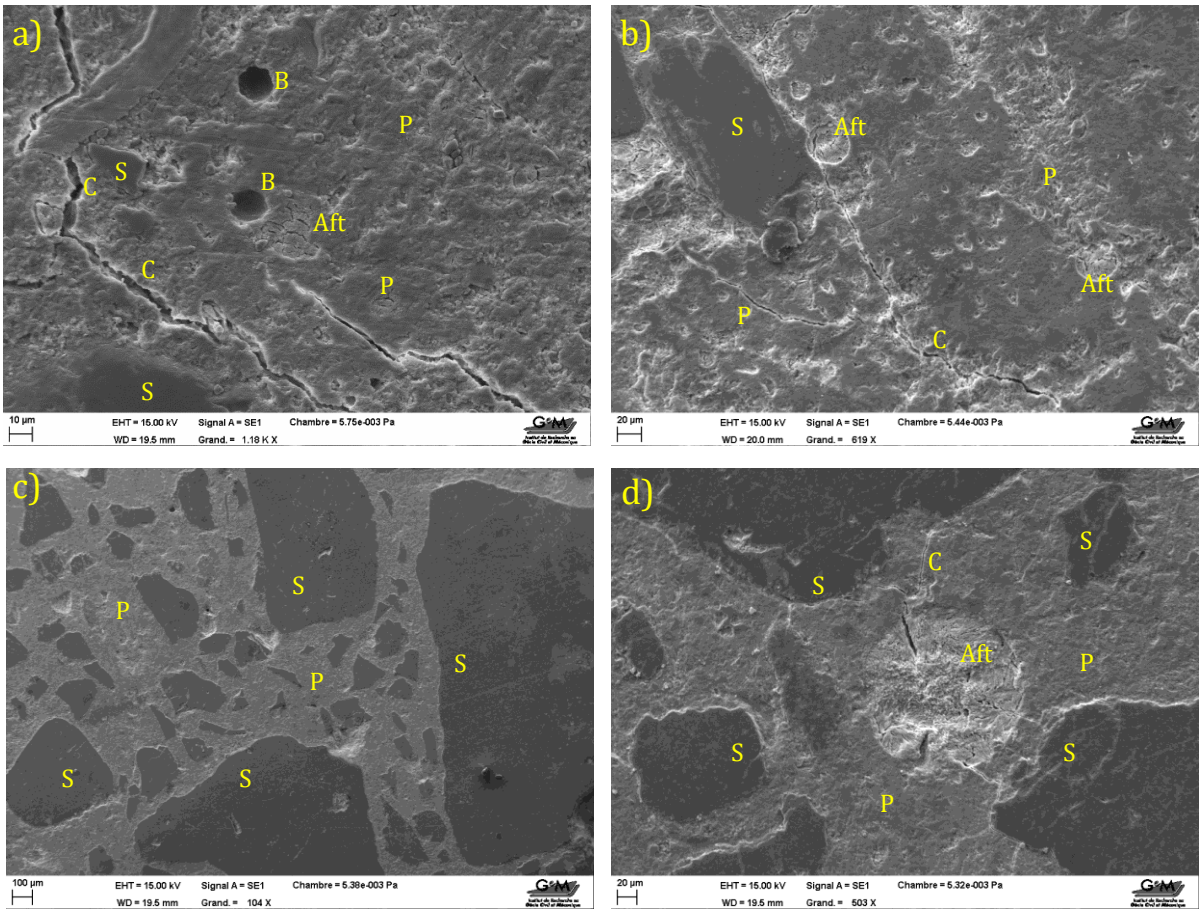

Figure 21– SEM image on "Qpr" (a), "Prs" (b) and "Ref" (c and d) samples at 360 days; expansion : 0.04% (a), 0.03% (b) and 0.02 (c and d). Ettringite found in air bubbles in "Qpr" and "Prs" and rarely in "Ref" paste. (P: Paste, S: Sand, C: Crack, Aft: Ettringite, B: air bubble).

3.2. Effect of gypsum plaster powder pollution

Plaster powder was used to imitate sulphate pollution in RCA. Four mortar mixtures using polluted RCS have been studied for DEF development and they have been compared to plaster free RCS mortars (see 2.2.1). In this part, the RCS formulations, "Qpr" and "Prs" tests results will be compared to the results of 4 formulations made of polluted sands using plaster powder.

3.2.1. Expansion, mass uptake and dynamic modulus evolution

Plaster powder is mainly composed of calcium sulphate dihydrate ($CaSO_4;2H_2O$) which could enhance DEF development. According to the results shown in Figure 24, the RCS mortars did not exhibit a significant expansion, additionally, the fine plaster powder is likely to decrease the expansion amplitude contrary to the expectations. "Qpr" and "Qpr-1.2CP" formulations have the highest expansion amplitude reaching an expansion of 0.04% while the third rank is for "Prs" mortar which is close to 0.04%. On the other hand, the three formulations incorporating the fine plaster powder, "Qpr-1.2FP", "Qpr-0.8FP" and "Prs-1.2FP" reached only 0.02%. The mass uptake is close in all formulations reaching 3 to 4% in one year of water immersion. However higher water mass uptake had been found in sodium sulphate added formulations (Figure 7: "Ref-SS", "Qpr-SS" and "Prs-SS") which is about 4.5% at the age of one year.

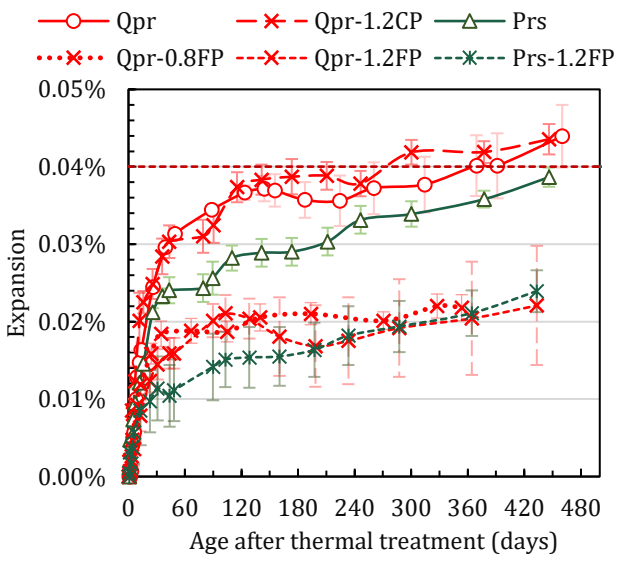

Figure 22– Expansion of the 6 RCS aggregate mortars with or without plaster pollution.

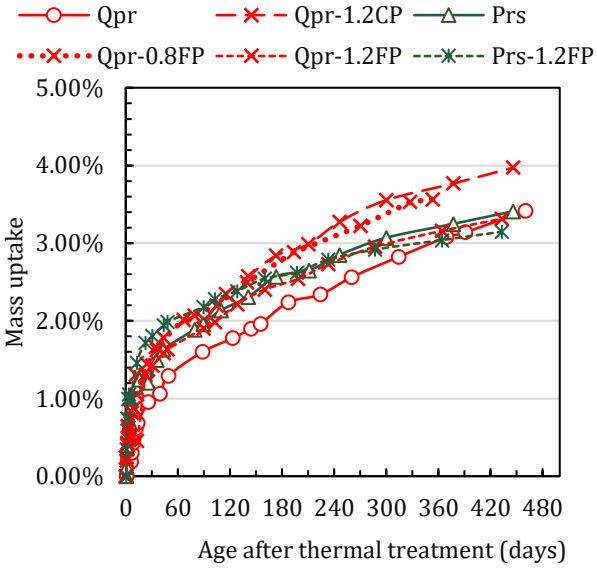

Figure 23– Mass uptake of the 6 RCS aggregate mortars with or without plaster pollution.

The dynamic Young modulus shown in Figure 26 shows an increase in stiffness of the mortars made by recycled sand mostly at early-age which indicates a continuous hydration of the remaining anhydrous clinker. Additionally, no sign of stiffness loss is noticed, hence the following formulations did not develop any significant DEF symptoms. Mortars made of Paris sand have higher stiffness than the mortars of Quimper sand. This difference is attributed to the higher paste proportion and higher absorption in Quimper sand than in Paris sand (Table 4). Mortars with plaster powder have slightly higher stiffness at early-age than plaster free mortars. Moreover, dynamic Young modulus variation in Figure 27 shows that the fine plaster powder limits the subsequent stiffness augmentation which is the result of the inhibition of cement hydration by calcium sulphate. The fine plaster powder is more soluble and has higher impact on cement hydration than the coarse plaster powder.

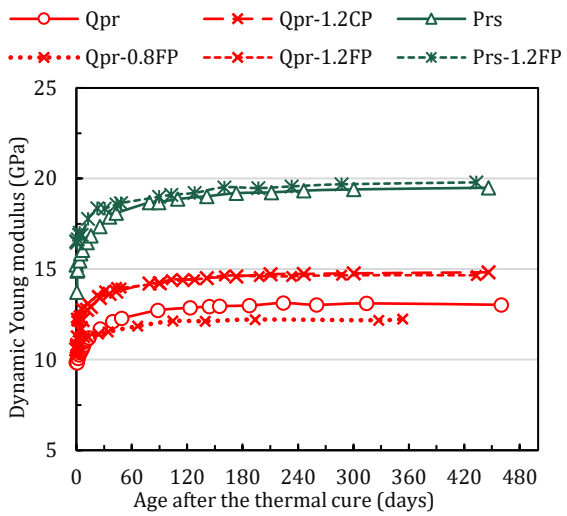

Figure 24– Dynamic modulus evolution of the 6 RCS aggregate mortars with or without plaster pollution.

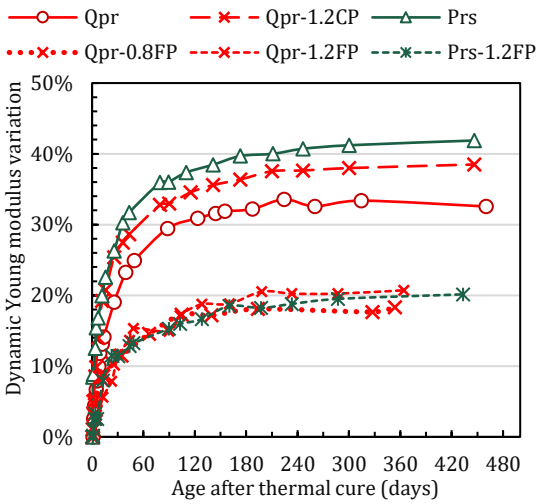

Figure 25– Variation of the dynamic modulus for the 6 RCS aggregate mortars.

3.2.2. Porosity and pore size distribution

Porosity and the skeletal density of the six mortars ("Qpr", "Prs", "Qpr-1.2CP", "Qpr-1.2FP", "Qpr-0.8FP" and "Prs-1.2FP") are shown in Figure 28. The porosity results fluctuate for each mortar without any particular reason and this variation has been explained before in § 3.1.2 as linked to the inability to fully saturated the pores of the mortar in 48 hours which is the mentioned duration in NF P 18-459 standard [44]. Moreover, this problem is noticed to happen in mortars made of RCS and far less with the reference mortar which could be attributed to a largely higher porosity in the mortars made of RCS as compared to the reference mortars. Higher porous volume needs more time to be fully saturated during the water immersion at low pressure. The variation in the skeletal density further evidence this porosity test bias. According to the results, little difference is found in porosity between the mortars made of Quimper sand without additions and mortars with plaster powder. The difference in porosity of mortars made of Paris sand with or without plaster powder is more pronounced, at 28 days "Prs" had a porosity of 30.8% versus 32.4% for "Prs-1.2FP". This difference of 2 to 3% of porosity is confirmed at 90 days, 180 days. At 360 days "Prs" porosity was 30.9% while "Prs-1.2FP" was 34.1%. This evolution is however not significant and is mostly due to the problem of water accessibility to the pores during this test. This bias is again confirmed on the skeletal density graph of "Prs-1.2FP" that increases from 28 days to 180 days and decreases from 180 days to 360 days.

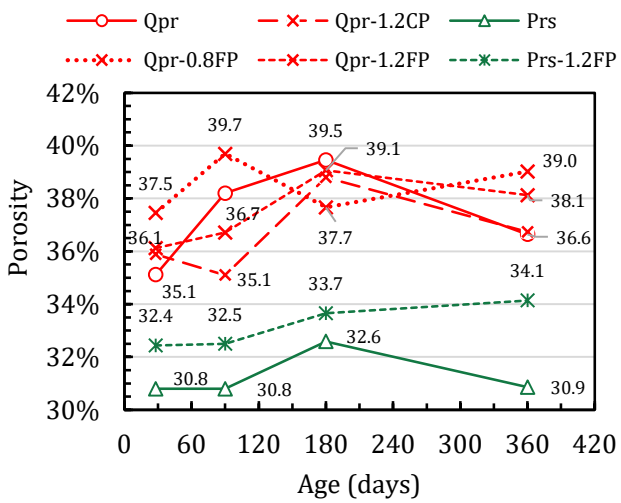

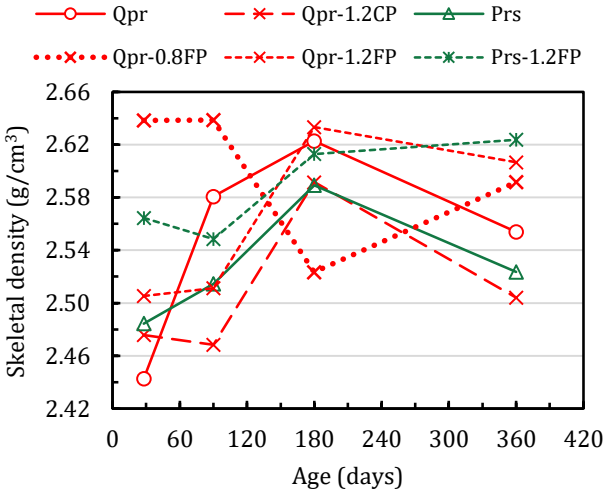

Figure 26– Porosity and skeletal density evolution of the 6 RCS aggregate mortars with or without plaster pollution.

The pore size distribution for the three mortars ("Qpr-1.2CP", "Qpr-1.2FP" and "Prs-1.2FP") at 28 and 180 days are shown in Figure 29. Pore size distribution is similar between the three mortars with plaster powder and the mortars without additions in Figure 12. The maximum pore size density is around 100 nanometers at 28 days for the three mortars, and this peak shift towards smaller pore sizes after 180 days of water immersion. The displacement of the porous distribution to small pores has been identified (§ 3.1.2) in all mortars regardless of their development of DEF symptoms or not. The displacement in the pore size distribution to smaller diameter could be the result of ongoing hydration as well as diffusion of ions from nanometric pores to micrometric ones when ettringite dissolves according to the proposed theory of Scherer [53] on ettringite crystallization. DEF development depends on crystallization pressures of ettringite in pores, which are not always sufficiently elevated to develop damage. Crystallization depends on pore diameter and on the volume of pores that are subjected to crystallization. In case where a large volume of small pores exist, which is the case of RCS mortars, the quantity of ettringite will not be enough to fill the small pores and this could decrease the crystallization pressure by lowering the concentration of ions in the solution.

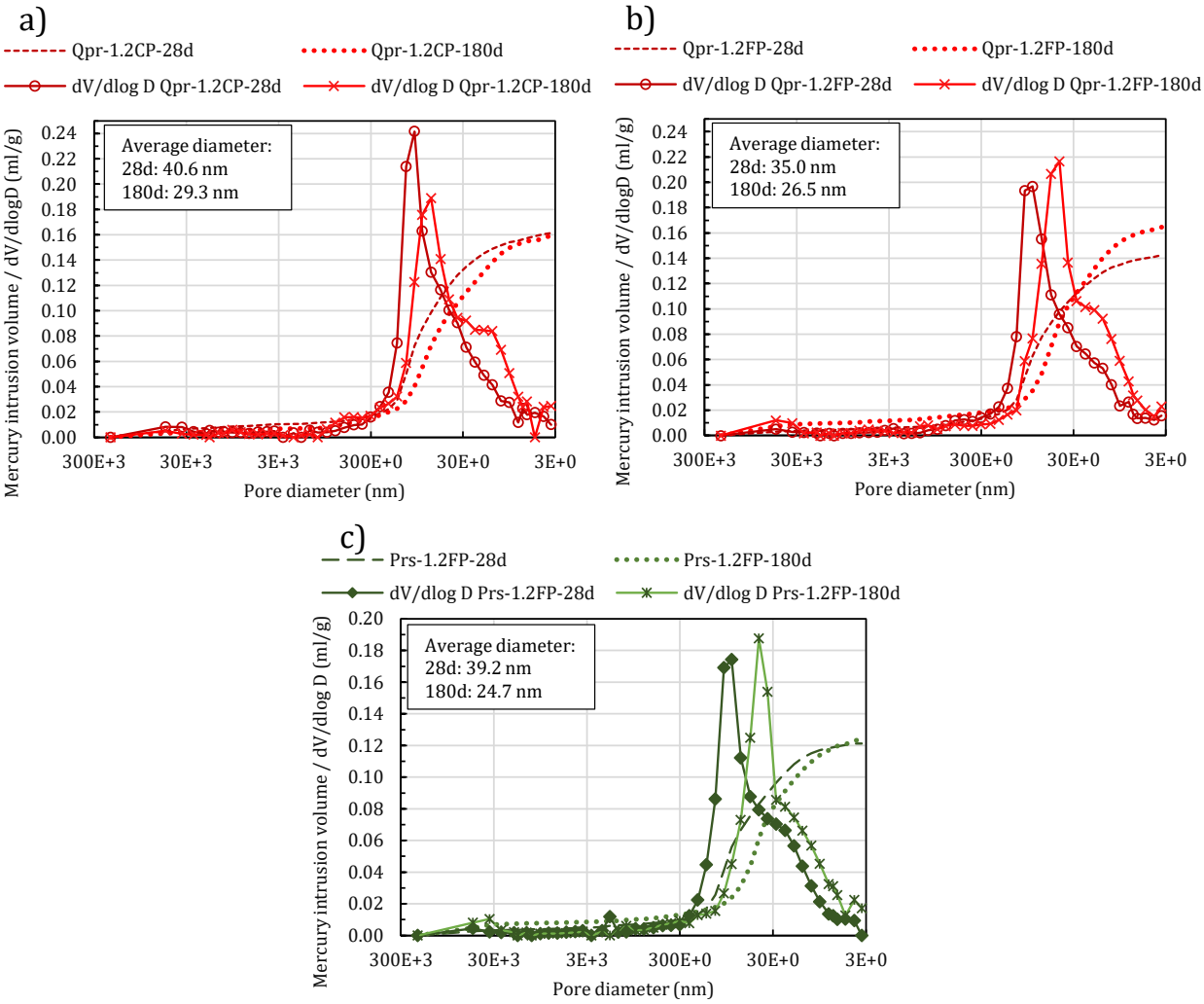

Figure 27– Pore size distribution for the three formulations: (a) "Qpr-1.2CP", (b) "Qpr-1.2FP" and (c) "Prs-1.2FP" at 28 and 180 days.

3.2.3. Mortar compressive and tensile strength

Compressive and tensile strength of the mortars made of recycled sand are shown in Figure 30. Mortars with Quimper sands have the lowest strength regardless of the amount of plaster powder used and its fineness. The compressive and the tensile strength increases from 28 days till 360 days in all formulations which indicates that hydration is still ongoing. The evolution in compressive strength is modified when plaster powder is used, especially for the fine plaster powder. In the two formulations "Qpr-1.2FP" and "Qpr-0.8-FP" the compressive strength is 22.4 MPa at 28 days which is higher than in "Qpr" formulation having a compressive strength of 16.7 MPa at 28 days. The strength of "Qpr-1.2FP" and "Qpr-0.8-FP" increases a little and reaches 24 MPa at one year while the "Qpr" mortar reaches 26.5 MPa. The mortar with the coarse plaster powder ("Qpr-1.2CP") had a different strength evolution from the other three mortars, the initial strength (21.4 MPa) was in between the plaster powder free and the added plaster powder mortars but at one year it reached the highest value (27.8 MPa) in this category of sand. The fine plaster powder had a similar effect in "Prs-1.2FP" mortar. The initial value of compressive strength (31.8 MPa) of "Prs-1.2FP" mortar is higher than the strength of "Prs" mortar (30.2 MPa) but at 360 days, plaster free mortar "Prs" had 38.3 MPa while "Prs-1.2FP" mortar had 34.8 MPa. Tensile strength is impacted by the plaster powder but not as much as the compressive strength. According to Barbosa et al. [56] many studies have evaluated the interaction between C_3A and gypsum that is added in cements to control concrete setting time [57,58]. Hydration kinetics is influenced by calcium sulphate reactivity which depends on the crystalline nature of calcium sulphate and its solubility which is related to its fineness. Furthermore, C-S-H growth seems to be modified by gypsum content. Quennoz and Scrivener [59] found an acceleration of alite (C_3S) hydration when tricalcium aluminate and gypsum were added to a pure mixture of alite and water. In this study, gypsum free mortars with recycled sand showed low initial mechanical characteristics at 28 days compared to mortars with fine plaster powder but after one year of conservation, the mechanical characteristics of gypsum free mortars scored better than fine gypsum added mortars. Initial mechanical characteristics seem to be higher in fine gypsum added mortars which could be attributed to an acceleration in hydration of some cement compounds [59]. At long term, some cement compounds will remain much more abundant in mortars without additions. These compounds hydrate at a later stage enhancing the mechanical characteristics of addition free mortars.

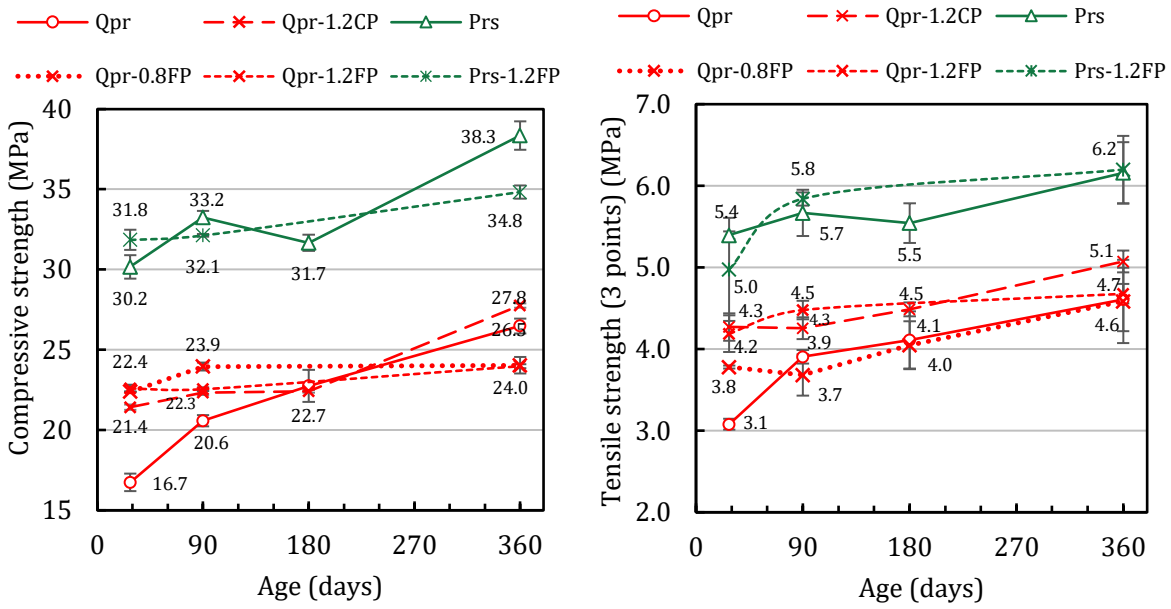

Figure 28– Mortar compressive and tensile strength evolution for the six mortars made of RCS.

3.2.4. Gas permeability

Figure 31 shows the evolution of the intrinsic permeability of the six mortars ("Qpr", "Prs", "Qpr-1.2CP", "Qpr-1.2FP", "Qpr-0.8FP" and "Prs-1.2FP"). Permeability is around 10^{-16} m^2 for all mortars. No remarkable evolution is noticed after one year, a small decrease is measured after 180 days except for "Qpr". Permeability values constitute a solid proof that no DEF damage developed in these mortars.

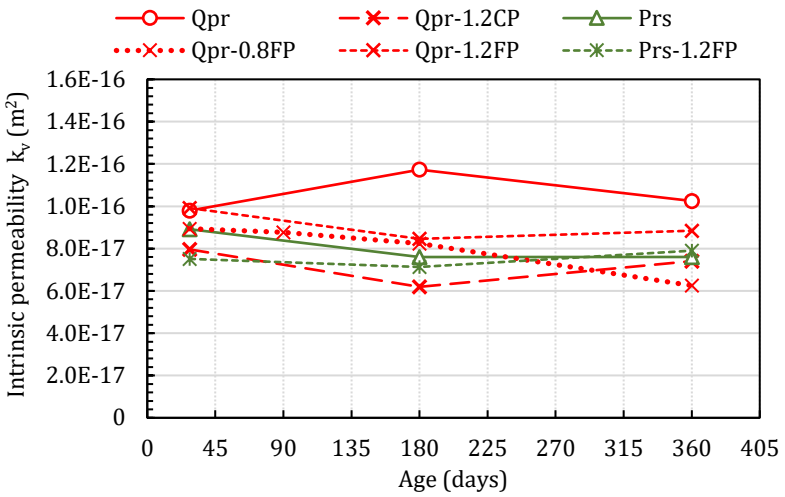

Figure 29– Evolution of the intrinsic permeability of the six mortars made of RCS.

3.2.5. SEM observations

SEM images in Figure 32 shows the same aspects of ettringite crystallization in air micro bubbles than found in SEM images in Figure 21 and in Figure 23. It is not clear whether the amount of ettringite formed in the plaster added mortars is greater than that of non-added mortars. The ITZ is free from massive ettringite crystallization and there is so any sign of debonding between the paste and the aggregates. The double interface composed of the old paste/natural aggregate interface and the old paste/new paste interface is not precisely detected. The mineralogical similarities between the two pastes makes their interface identification difficult.

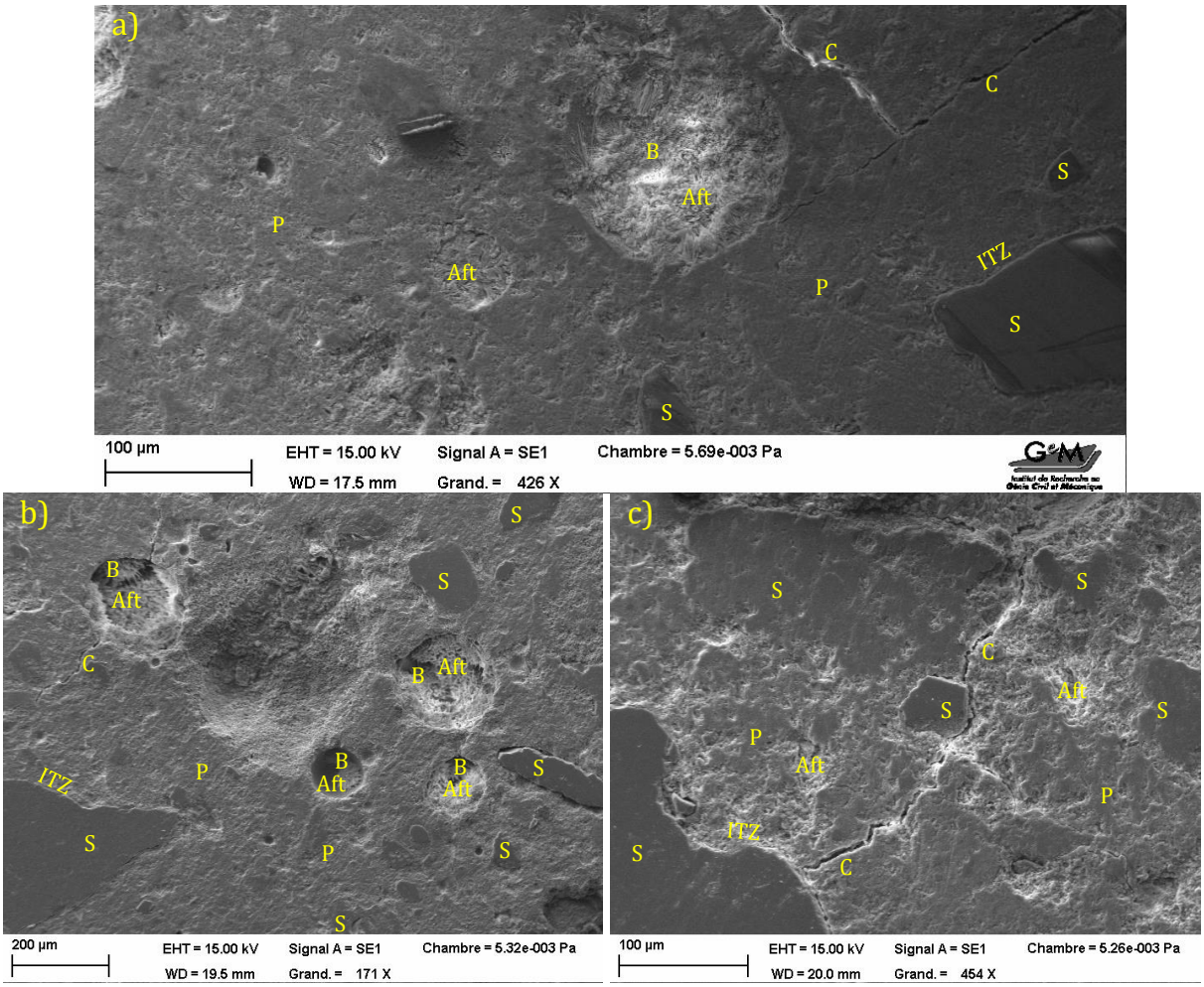

Figure 30– SEM image on "Qpr-1.2CP" (a), "Qpr-1.2FP" (b) and "Prs-1.2FP" (c) samples at 360 days; expansion : 0.04% (a), 0.02% (b) and 0.02 (c). (P: Paste, S: Sand, C: Crack, Aft: Ettringite, B: air bubble).

4. Conclusions

In this study, several recycled sand based mortars using two different recycled sands were studied for delayed ettringite formation and compared to reference mortars made with standardised siliceous sand. The obtained results lead to the following conclusions:

a) Impact of sodium sulphate addition:

Three mortar formulations, a standardised siliceous sand based mortar and two recycled sand based mortars were done using sodium sulphate addition and compared to their mortar formulation counterparts without additions. Sodium sulphate at 5% SO_3 by cement weight accelerated and amplified DEF expansion and microcracking in standardised siliceous based mortar and to a much lesser extent, in one RCA sand based mortar. Mineralogical nature of recycled sand impacts DEF development. The recycled sand that comprised 60% of quartz and one-tenth feldspar induced an expansion while the one comprising one-third limestone did not induce DEF related expansion. Limestone powder could inhibit the formation of ettringite by consuming aluminates, this reaction produces calcium carboaluminate. Expansion was found to be largely higher in standardised sand based mortars than in recycled sand based mortars. After one year, permeability increased 100 times in the standardised based mortars, 5 times in the mortar made of recycled sand where DEF appeared while it did not change in the recycled sand based mortar with no DEF expansion. A high correlation is noticed between expansion and permeability except for the reference mortar without additions that developed macrocracking in permeability samples (cylindrical samples) while no expansion was measured on prismatic samples.

b) Impact of gypsum plaster powder additions:

Four mortar formulations with gypsum plaster powder pollution were studied for sulphate attack. Two mortars included fine gypsum plaster powder at 1.2% sulphate by weight of sand, a mortar with coarse plaster powder pollution at 1.2% and a mortar with fine plaster at 0.8%. Results show that plaster powder had little impact on DEF expansion (≤0.05%). Fine plaster powder induced lower expansion (≤0.02%) than pollution-free recycled sand based mortars or mortar with coarse plaster powder. Fine plaster powder limited dynamic modulus and compressive resistance augmentation. This could be explained by the inhibition impact of plaster on cement hydration. No permeability evolution is noticed in mortars made of recycled sands without additions or with plaster pollution.

c) Impact of recycled sand in mortars regarding sulphate attack:

The use of recycled sands in mortar reduces or could completely negate the expected expansion of an internal sulphate attack. Recycled sand can entrain air bubbles of 10 to 100 micrometres size in cement paste during mixing. Fine particles found in important quantities in recycled aggregates are probably responsible for the entrainment effect. Ettringite ions that are in super-concentration move easily in large amount of porous volume and crystallises freely without expansive pressure. Microbubbles behaves like ion pumps, they pump all the sources of super-concentration until they are empty, and thereafter no noticeable expansion will appear. The same phenomena was described in air entrained concrete where DEF expansion decreased with higher entrained air volume [55]. Recycled sand based mortars are just capable of producing ettringite as siliceous sand based mortars, but their ability to entrain air reduces the risk of developing DEF damage. However, replacing the standardised sand by recycled sands in mortars impacts negatively the mechanical characteristics of mortars, particularly the compressive strength and the dynamic Young modulus. A decrease of 50 to 65 % in the dynamic Young modulus and 20 to 60% in the compressive strength is observed in comparison to the standardised sand based mortars.

d) Concerning the actual standards and their limitations for using RCA

The European standard [NF EN 12620] and many other standards have established a limit of sulphate content for recycled aggregate ranging from the strictest one; 0.2% for the European standard and up to 1% in the case of the British code. These limits are mostly below the concentration used in this study. The recycled sand based mortars with a sulphate content of 1.2% showed very little damage in the case where the aggregate was rich in alkaline and was composed mostly of siliceous natural aggregate. No damage is noticed when the RCA sand was low in alkaline and rich in limestone natural aggregate. According to our results, there should be a possibility to increase the limit of sulphate in recycled aggregates mostly when they have a low alkaline content and when their natural aggregate phase is largely composed of limestone.

Furthermore, higher sulphate concentrations and lower entrained air formulations should be studied to establish a correlation between the amount of entrained air and the expected expansion mortars made of recycled sands.

5. Acknowledgement

The authors would like to acknowledge:

- The Algerian-French cooperation project Tassili 19MDU216.
- The financial support of the Polish National Agency for Academic Exchange under the International Academic Partnership Program: PPI/APM/2018/1/00027 *E-mobility and sustainable materials and technologies* EMMAT.

Bibliography

[1] ilker B. Topçu, N.F. Günçan, Using waste concrete as aggregate, Cem. Concr. Res. 25 (1995) 1385–1390. https://doi.org/10.1016/0008-8846(95)00131-U.

[2] S. Chandra, Implications of using recycled construction demolition waste as aggregate in concrete, in: Sustain. Waste Manag. Recycl. Constr. Demolition Waste, n.d.: pp. 104–114. https://doi.org/10.1680/cdw.32859.0011.

[3] J.-L. Gálvez-Martos, D. Styles, H. Schoenberger, B. Zeschmar-Lahl, Construction and demolition waste best management practice in Europe, Resour. Conserv. Recycl. 136 (2018) 166–178. https://doi.org/10.1016/j.resconrec.2018.04.016.
[4] F. de Larrard, H. Colina, Le béton recyclé, Ifsttar, Marne-la-Vallée, 2018.
[5] R.V. Silva, J. de Brito, R.K. Dhir, Properties and composition of recycled aggregates from construction and demolition waste suitable for concrete production, Constr. Build. Mater. 65 (2014) 201–217. https://doi.org/10.1016/j.conbuildmat.2014.04.117.
[6] H.F.W. Taylor, C. Famy, K.L. Scrivener, Delayed ettringite formation, Cem. Concr. Res. 31 (2001) 683–693. https://doi.org/10.1016/S0008-8846(01)00466-5.
[7] Y. Fu, J.J. Beaudoin, Microcracking as a precursor to delayed ettringite formation in cement systems, Cem. Concr. Res. 26 (1996) 1493–1498. https://doi.org/10.1016/0008-8846(96)00134-2.
[8] R. Barbarulo, H. Peycelon, S. Prené, The role of CSH and temperature in delayed ettringite formation, in: Int. RILEM TC 186-ISA Workshop Intern. Sulfate Attack Delayed Ettringite Form., 2002: pp. 155–166.
[9] K. Scrivener, D. Damidot, C. Famy, Possible Mechanisms of Expansion of Concrete Exposed to Elevated Temperatures During Curing (Also Known as DEF) and Implications for Avoidance of Field Problems, (1999).
[10] M. Salgues, A. Sellier, S. Multon, E. Bourdarot, E. Grimal, DEF modelling based on thermodynamic equilibria and ionic transfers for structural analysis, Eur. J. Environ. Civ. Eng. 18 (2014) 377–402. https://doi.org/10.1080/19648189.2013.872579.
[11] R.J. Flatt, G.W. Scherer, Thermodynamics of crystallization stresses in DEF, Cem. Concr. Res. 38 (2008) 325–336. https://doi.org/10.1016/j.cemconres.2007.10.002.
[12] N. Leklou, Contribution to the knowledge of internal sulphate reaction, PhD Thesis, L'université Paul Sabatier Toulouse, 2008. https://hal.archives-ouvertes.fr/tel-01086605.
[13] S. Sahu, N. Thaulow, Delayed ettringite formation in Swedish concrete railroad ties, Cem. Concr. Res. 34 (2004) 1675–1681. https://doi.org/10.1016/j.cemconres.2004.01.027.
[14] A. Awasthi, K. Matsumoto, K. Nagai, S. Asamoto, S. GOTO, Investigation on possible causes of expansion damages in concrete – a case study of sleepers in Indian Railways, J. Asian Concr. Fed. 3 (2017) 49–66. https://doi.org/10.18702/acf.2017.06.3.1.49.
[15] Y. Amine, N. Leklou, O. Amiri, Effects of Ternary Cements with Limestone Filler on DEF in Concrete, Spec. Publ. 320 (2017).
[16] V.-H. Nguyen, N. Leklou, J.-E. Aubert, P. Mounanga, The effect of natural pozzolan on delayed ettringite formation of the heat-cured mortars, Constr. Build. Mater. 48 (2013) 479–484. https://doi.org/10.1016/j.conbuildmat.2013.07.016.
[17] N. Leklou, J.-E. Aubert, G. Escadeillas, Microscopic observations of samples affected by delayed ettringite formation (DEF), Mater. Struct. 42 (2008) 1369. https://doi.org/10.1617/s11527-008-9456-9.
[18] Z. Zhang, J. Olek, S. Diamond, Studies on delayed ettringite formation in heat-cured mortars: II. Characteristics of cement that may be susceptible to DEF, Cem. Concr. Res. 32 (2002) 1737–1742. https://doi.org/10.1016/S0008-8846(02)00894-3.
[19] N. Leklou, J.-E. Aubert, G. Escadeillas, Influence of various parameters on heat-induced internal sulphate attack, Eur. J. Environ. Civ. Eng. 17 (2013) 141–153. https://doi.org/10.1080/19648189.2012.755338.
[20] J.-E. Aubert, G. Escadeillas, N. Leklou, Expansion of five-year-old mortars attributable to DEF: Relevance of the laboratory studies on DEF?, Constr. Build. Mater. 23 (2009) 3583–3585. https://doi.org/10.1016/j.conbuildmat.2009.08.015.
[21] R. Yang, C.D. Lawrence, J.H. Sharp, Effect of type of aggregate on delayed ettringite formation, Adv. Cem. Res. 11 (1999) 119–132. https://doi.org/10.1680/adcr.1999.11.3.119.
[22] M.S. de Juan, P.A. Gutiérrez, Study on the influence of attached mortar content on the properties of recycled concrete aggregate, Constr. Build. Mater. 23 (2009) 872–877. https://doi.org/10.1016/j.conbuildmat.2008.04.012.
[23] M. Etxeberria, E. Vázquez, A. Marí, M. Barra, Influence of amount of recycled coarse aggregates and production process on properties of recycled aggregate concrete, Cem. Concr. Res. 37 (2007) 735–742. https://doi.org/10.1016/j.cemconres.2007.02.002.
[24] AFNOR NF EN 206/CN, Béton — Spécification, performance, production et conformité — Complément national à la norme NF EN 206, AFNOR Editions, 2014.
[25] AFNOR NF EN 12620+A1, Granulats pour le béton, AFNOR Editions, 2008.
[26] AFNOR NF EN 1744-1+A1, Essais visant à déterminer les propriétés chimiques des granulats - Partie 1 : analyse chimique, AFNOR Editions, 2014.
[27] Instrucción de Hormigón Estructural EHE-08, Spain: Ministerio de Fomento, 2008.

[28] Bogue RH, Calculation of the compounds in Portland Cement., Ind Eng Chem Anal Ed., 1929.
[29] P. Rougeau, L. Schmitt, J. Nai-Nhu, A. Djerbi, M. Saillio, E. Ghorbel, J.-M. Mechling, D. Bulteel, M. Cyr, A. Lecomte, N. Leklou, R. Trauchessec, I. Moulin, T. Lenormand, O. Amiri, Propriétés liées à la durabilité, in: Béton Recyclé, Ifsttar, De Larrard F. et Colina H., Marne-la-Vallée, 2018.
[30] V.H. Nguyen, Effets d'additions minérales sur l'apparition de la Réaction Sulfatique Interne : étude paramétrique, développement et optimisation de méthodes accélérées, PhD Thesis, Université de Nantes, 2013.
[31] A. Pavoine, Evaluation du potentiel de réactivité des bétons vis-à-vis de la formation différée de l'ettringite, PhD Thesis, 2003.
[32] G. Escadeillas, J.-E. Aubert, M. Segerer, W. Prince, Some factors affecting delayed ettringite formation in heat-cured mortars, Cem. Concr. Res. 37 (2007) 1445–1452. https://doi.org/10.1016/j.cemconres.2007.07.004.
[33] V.-H. Nguyen, N. Leklou, P. Mounanga, The effect of metakaolin on internal sulphate attack of the heatcured mortars, Romanian J. Mater. 49 (2019) 51–57.
[34] X. Brunetaud, R. Linder, L. Divet, D. Duragrin, D. Damidot, Effect of curing conditions and concrete mix design on the expansion generated by delayed ettringite formation, Mater. Struct. 40 (2007) 567–578. https://doi.org/10.1617/s11527-006-9163-3.
[35] AFNOR NF EN 206-1+A1, Béton — Spécification, performances, production et conformité, AFNOR Editions, 2016.
[36] AFNOR NF P18-594, Granulats - Méthodes d'essai de réactivité aux alcalis, AFNOR Editions, 2015.
[37] AFNOR NF EN 1097-6, Essais pour déterminer les caractéristiques mécaniques et physiques des granulats - Partie 6 : détermination de la masse volumique réelle et du coefficient d'absorption d'eau, AFNOR Editions, 2014.
[38] LCPC, Méthode d'essai LPC N°37 : Essai de granulats. Détermination des alcalins solubles dans l'eau de chaux, LCPC, Paris, 1993.
[39] F. Delobel, D. Bulteel, J.M. Mechling, A. Lecomte, M. Cyr, S. Rémond, Application of ASR tests to recycled concrete aggregates: Influence of water absorption, Constr. Build. Mater. 124 (2016) 714–721. https://doi.org/10.1016/j.conbuildmat.2016.08.004.
[40] R.-P. Martin, Experimental analysis of concrete structures affected by delayed ettringite formation, PhD Thesis, Université Paris-Est, 2010. https://pastel.archives-ouvertes.fr/tel-00558200.
[41] AFNOR NF P18-452, Bétons - Mesure du temps d'écoulement des bétons et des mortiers au maniabilimètre, AFNOR Editions, 2017.
[42] AFNOR NF EN ISO 12680-1, Méthodes d'essai pour produits réfractaires - Partie 1 : détermination du module de Young dynamique (MOE) par excitation de vibration par impulsion, AFNOR Editions, 2007.
[43] ASTM E1876 - 15, Standard Test Method for Dynamic Young's Modulus, Shear Modulus and Poisson's Ratio by Impulse Excitation of Vibration, n.d.
[44] AFNOR NF P 18-459, Béton - Essai pour béton durci - Essai de porosité et de masse volumique, AFNOR Editions, 2010.
[45] A. Ben Fraj, S. Bonnet, A. Khelidj, Effect of slag on transfer parameters and chloride binding isotherms of concrete, in: Concreep'8, Nagoya, Japan, 2008. https://hal.archives-ouvertes.fr/hal-01978524.
[46] N. Leklou, J.-E. Aubert, G. Escadeillas, Microscopic observations of samples affected by delayed ettringite formation (DEF), Mater. Struct. Constr. 42 (2009) 1369–1378. https://doi.org/10.1617/s11527-008-9456-9.
[47] N. Leklou, J.-E. Aubert, G. Escadeillas, Effect of wetting-drying cycles on mortar samples affected by DEF, Eur. J. Environ. Civ. Eng. 16 (2012) 582–588. https://doi.org/10.1080/19648189.2012.668017.
[48] LCPC, Recommandations pour la prévention des désordres dus à la réaction sulfatique interne, LCPC, Paris, 2007.
[49] M. Al Shamaa, S. Lavaud, L. Divet, G. Nahas, J.M. Torrenti, Influence of relative humidity on delayed ettringite formation, Cem. Concr. Compos. 58 (2015) 14–22. https://doi.org/10.1016/j.cemconcomp.2014.12.013.
[50] N. Leklou, V.H. Nguyen, P. Mounanga, The effect of the partial cement substitution with fly ash on Delayed Ettringite Formation in heat-cured mortars, KSCE J. Civ. Eng. 21 (2017) 1359–1366. https://doi.org/10.1007/s12205-016-0778-9.
[51] A. Yammine, F. Bignonnet, N. Leklou, M. Choinska, T. Stryszewska, Micromechanical modelling of damage induced by delayed ettringite formation, in: Bayonne, France, 2019. https://doi.org/doi.org/10.21012/FC10.233150.
[52] A. Yacoub, A. Djerbi, T. Fen-Chong, The effect of the drying temperature on water porosity and gas permeability of recycled sand mortar, Constr. Build. Mater. 214 (2019) 677–684. https://doi.org/10.1016/j.conbuildmat.2019.04.128.

[53] G.W. Scherer, Stress from crystallization of salt, Cem. Concr. Res. 34 (2004) 1613–1624. https://doi.org/10.1016/j.cemconres.2003.12.034.
[54] V. Picandet, A. Khelidj, G. Bastian, Effect of axial compressive damage on gas permeability of ordinary and high-performance concrete, Cem. Concr. Res. 31 (2001) 1525–1532. https://doi.org/10.1016/S0008-8846(01)00546-4.
[55] N. Petrov, Effets combinés de différents facteurs sur l'expansion des bétons causée par la formation différée d'ettringite, PhD Thesis, Université de Sherbrooke, 2003.
[56] W. Barbosa, R.D. Ramalho, K.F. Portella, Influence of gypsum fineness in the first hours of cement paste: Hydration kinetics and rheological behaviour, Constr. Build. Mater. 184 (2018) 304–310. https://doi.org/10.1016/j.conbuildmat.2018.06.235.
[57] G. Tzouvalas, N. Dermatas, S. Tsimas, Alternative calcium sulfate-bearing materials as cement retarders: Part I. Anhydrite, Cem. Concr. Res. 34 (2004) 2113–2118. https://doi.org/10.1016/j.cemconres.2004.03.020.
[58] H. Zhang, Z. Lin, D. Tong, Influence of the type of calcium sulfate on the strength and hydration of portland cement under an initial steam-curing condition, Cem. Concr. Res. 26 (1996) 1505–1511. https://doi.org/10.1016/0008-8846(96)00149-4.
[59] A. Quennoz, K.L. Scrivener, Interactions between alite and C3A-gypsum hydrations in model cements, Cem. Concr. Res. 44 (2013) 46–54. https://doi.org/10.1016/j.cemconres.2012.10.018.